博士学位論文

転写因子 Runx2 の近位プロモーター誘導型アイソフォームの骨形成への影響の解析

東京大学大学院　新領域創成科学研究科　メディカルゲノム専攻

東京大学医科学研究所　炎症免疫学分野

指導教員：　清野　宏　教授

入学年月日：　2010 年 4 月 1 日

学籍番号：　47-107326

氏名：　大倉　英明

Index

Abbreviation.....3

Part1

Introduction.....5

Materials and Methods.....13

Results.....31

Discussion.....48

References.....57

Part2

Introduction.....61

Materials and Methods.....68

Results.....79

Discussion.....87

References.....101

Acknowledgements.....105

Figures.....106

Abbreviation

NALT: Nasopharynx-Associated Lymphoid Tissue, IgA: Immunoglobulin A, SARS: Severe Acute Respiratory Syndrome, LTi: Lymphoid Tissue inducer, LTo: Lymphoid Tissue organizer, RORγt: Retinoic acid Orphan Receptor gamma t, Id2: Inhibitor of DNA-binding 2, IL-7R: Interleukin-7 Receptor, LTa: Lymphotoxin alpha, NFκB: Nuclear Factor kappa B, LTβR: Lymphotoxin beta Receptor, PPARγ: Peroxisome Proliferator-Activated Receptor gamma, CD: Cluster of Differentiation, FACS: Fluorescent Activated Cell Sorting, PP: Peryer's Patches, RNA: Ribonucleic Acid, IRF: Interferon Regulatory Factor, DNA: Deoxyribonucleic Acid, Cbf: Core-binding factor, PBS: Phosphate Buffered Saline, EtOH: Ethanol, EDTA: Ethylenediaminetetraacetic Acid, FCS: Fetal Calf Serum, NCS: Newborn Calf Serum, NA: sodium, PCR: Polymerase Chain Reaction, qPCR: quantitative Polymerase Chain Reaction, UV: Ultra Violet, TBST: Tris Buffered Saline tween20, HEK: Human Embryonic Kidney, I.P.: Immunoprecipitation, I.B.: Immunoblot, HRP: Horse Radish Peroxidase, IMSUT: Institute of Medical science University of Tokyo, SPF: Specific Pathogen Free, RCAI: Research Center for Allergy and Immunology, PNAd:

Peripheral Node Adrressin, HEV: High Endothelial Venules, CCD: Cleidocranial Displasia, RDH: Runt Homology Domain, BMP: Bone Morphology Protein, TGF-β: Transforming Growth Factor-beta, TNF-α: Tumor Necrosis Factor-alpha, KOH: potassium hydroxide, LED: Light Emitting Diode, μCT: micro Computed Tomography, α-MEM: alpha-Modified Eagle's Medium, MSC: Mesenchymal Stem cells, PC: Personal Computer

1.1 Introduction

Nasopharynx-Associated Lymphoid Tissue (NALT) is the lymphatic architecture located at the bottom of murine nasal cavity[1]. NALT consists of lymphoid and myeloid cells including B cell, T cell and dendritic cell which segregate to form zones of each cell[1,2]. NALT has been considered to be the immune inductive tissue because of the several lines of evidences such as the existence of antigen sampling M cells on the surface of NALT, formation of germinal center following the immunization by mucosal adjuvant Cholera Toxin and the occurrence of B cell class switch recombination evidenced by the detection of Iα-Cμ circular transcript and IgA^+ plasma cells which are responsible for suppression of commensal and pathogenic bacteria at mucosal sites[1,3].

Given that NALT is the immune inducing lymphoid tissue at the upper respiratory tract, understanding its precise roles and controlling them are of great value. Infectious agent via air way route, such as influenza and SARS, cause severe symptom to patients and recent mutation of influenza into uncontrollable type suggests that novel strategy for prevention of its infection is more desirable than treatment after infection. Allergic responses

against pollen are also great loss of our society every year. To control allergic responses at upper air way needs correct comprehension of immune induction mechanism at the site of inflammation.

NALT is classified into the secondary lymphoid tissue which isn't, unlike primary lymphoid tissues such as bone marrow or thymus, involved in development of lymphocytes but is responsible for immunosurveillance of periphery[1]. The developmental mechanism of secondary lymphoid tissues has long been a target of intensive researches and well established. Two major players of secondary lymphoid tissue genesis are lymphoid tissue inducer cells (LTi) and lymphoid tissue organizer cells (LTo)[4]. Precursors of LTi reside in livers of fetuses and mature into LTi by the function of thymus related isoform of transcription factor Retioic-Acid Orphan Receptor gamma (RORγt) and Inhibitor of DNA-binding 2 (Id2)[1]. LTi cells have surface expression of Inter Leukin-7 Receptor (IL-7R), α4β7 integrin and membrane-bound Lymphotoxin alpha (LTα); receptor of growth signal from IL-7, adhesion molecule to stop and retain LTi at the lymphoid tissue anlagen, and the switch to activation of non-canonical NFκB pathway of LTo, respectively[4]. LTo expresses, after activation via LT beta Receptor (LTβR),

array of lymphoid chemokines and adhesion molecules that recruit and keep immunocompetent cells that are to form lymphoid tissue. Otherwise the LTo precursors develop into adipocytes under the instruction of PPARγ and Cebpα[5].

NALT formation is largely independent of these molecules involving in classical pathway of lymphoid tissue generation[6,7]. Previous reports showed NALT formation is abrogated but not completely lost in the gene knockout mice. Seemingly *Rorc*$^{-/-}$ mice have intact NALT[6]. *Il7r*$^{-/-}$, *Lta*$^{-/-}$, *Ltb*$^{-/-}$ and LTβR-Ig treated mice showed minimalized but obvious formation of lymphocyte aggregation at the site of NALT[7]. Despite them, Id2 deficient mice lacked NALT formation completely that suggested Id2 is indispensable for the development of NALT[7]. These results imply that NALT developmental pathway is different from those of other secondary lymphoid tissues in terms of requirement of transcription factors. In line with this insight, NALT formation begins 1 week after birth when other lymph nodes should have already progressed well[4]. Difference of initiation also suggests that there are distinctive mechanisms for the formation of NALT and other lymphoid tissues respectively.

To consider transcriptional regulation related to NALT, we have to examine LTi for NALT (NALT inducer; NALTi) because the most characteristic feature of NALT development is its independence of classical transcription factors involved in LTi development and function. LTi is classically defined as $CD3^-CD4^+CD45^+$ cell population[1]. This cell subset is recruited to the NALT anlagen at the initiation time point of NALT development, as observed by immunohistochemistry of frozen section of nasal tissue of day 10 mice[7]. When these cells were prepared from wild type mouse fetal livers or fetal intestines and adaptively transferred into *Id2*$^{-/-}$ mice, *Id2*$^{-/-}$ mice restored the NALT development to some extent, suggesting that these cell population triggers NALT formation[7]. By FACS analysis, however, it was revealed that NALTi express CD4 antigen at lower level (so classified as $CD3^-CD4^{low}CD45^+$ cells) than classical LTi ($CD3^-CD4^{high}CD45^+$ cells). Furthermore, when LTi from RORγt knockout mice, whose lymph node construction is largely defective but NALT formation is not affected, were examined, it showed lack of $CD3^-CD4^{high}CD45^+$ population but existence of $CD3^-CD4^{low}CD45^+$ NALTi, which is in consistent with intact NALT formation of these mice. Taken together, these previous results lead the emergence of

hypothesis that the organization of NALT and other lymphoid tissues is governed by distinctive LTi cell populations.

From results described above, our group compared the gene expression profiles of classical LTi and NALTi. In this case, small intestinal Peyer's Patches inducer cells (PPi) were used as representative classical LTi population. Both cell populations were purified from fetal intestines and d10 nasal tissue respectively, and mRNA was extracted from them. The subtractive gene comparison assay followed by differential display screening presented a number of candidate genes. Among them were two genes of the biggest expectation; IRF1 and P2Runx2.

Runx is the transcription factor that possesses Runt homology domain of Drosophila[8]. Runx2 is a one of Runx family transcription factors consist of three members; Runx1, Runx2 and Runx3, all of which have two major splicing variants, distal P1 and proximal P2[8]. Runx1 is well known by its relation to the lymphoid malignancy as the form of fusion protein Runx1-ETO[8]. It has quite many physiological roles such as the fate transition regulator from endothelial cell to haematopoietic cell[9], and the inducer and keeper of Foxp3 expression in the regulatory T cells[10-12]. Runx3

maintains cell proliferation in gastric mucosa and loss of function of it is the highly susceptible to epithelial hyperplasia[8]. Runx2 is mainly expressed in skeleton and known as the master regulator of bone formation[13-15], whereas there are a few reports about its function outside the bone[16], *e.g.* role for B cell class switch into IgA producing plasma cell together with Runx3[17].

Runx2 also has two isoforms generated by alternative splicing from P1 and P2 promoter region directed transcriptional regulation[18]. Both two isoforms share most part of their coding sequence. P2 isoform differs only by its N-terminal 5 amino acids from P1 counterpart. These two variants show most prominent difference in their expression pattern in the body. While P1 is strictly restricted in skeletal tissues, P2 spreads into various tissues and cells including brain, sperm and lymphocytes[19,20]. Given that P1 is for bone and P2 is for whole body, it is plausible that our previous finding was Runx2 of P2 isoform.

Runx transcription factors work with the aid of their partner Cbfβ that binds Runx and confers sufficient binding affinity to the Runx binding nucleotide motif (R/TACCRCA) on them[8]. Though Cbfβ doesn't have DNA binding domain and it works through modification of tertiary structure of

Runx[21], lack of Cbfβ result in many dysfunction in the body such as bone malformation[22-24], severe decrement of γδ T cell[25] and autoimmune disease like phenotype owing to the defective regulatory T cell maintenance[10,11]. These disorders were supposed to reflect functions of Runx family transcription factors, which are necessary for Cbfβ to regulate gene transcriptions. Cbfβ has two major functional splicing variants Cbfβ1 and Cbfβ2[26]. In these two isoforms, Cbfβ2 deficient mice showed defective NALT formation in our previous results. Actually, although it was reported that Cbfβ2 is involved in Peyer's Patches formation together with P1Runx1[26], P1Runx1 knockout mice didn't show any abnormality in NALT formation. This observation also supports the idea that P2Runx2 has some roles during the developmental period of NALT, especially in the maturation of NALTi.

There have not been reported the establishment of *in vitro* model that mimic fetal and neonatal lymphoid tissue development, analyzing lymph node construction needs suitable mouse models. So I was to establish Runx2 diminished mouse in order to address how P2Runx2 works in lymphoid tissue development. In spite of the incomplete vector recombination into genome, I managed to obtain the P2Runx2 diminished

mouse. Because the established mouse showed neonatal lethality, I searched the cause of lethality. Neomycin resistant gene cassette (*neo*^{r}), which was inserted into mouse genome as a selection marker, was prepared to be removed by flanking with loxP. Therefore, I excised it from genome in whole body at first. This reversed the lethality completely. Based on this result, I assumed that the insertion of *neo*^{r} is the cause of lethality and found that *neo*^{r} generated Runx2-neo^r fusion mRNA. *Neo*^{r} also made fusion transcripts with P1Runx2. Therefore, unfortunately, the established mouse was revealed not to be P2 isoform specific knockout. Nevertheless, considering tissue specific expression patterns of these isoforms, this mouse can be used as P2Runx2 knockout in NALT genesis. In order to rescue lethality, I removed *neo*^{r} in whole body or chondrocyte specifically only to find that the NALT generation was independent of P2Runx2. Moreover, I found NALT-like lymphoid aggregates in previously reported "NALT deficient" mice. Based on these results, I decided to quit this project.

1.2 Materials and Methods

1.2.1 *Mouse*

C57BL/6J mice were purchased from CLEA Japan Inc. *Rorc*$^{-/-}$ mice were gifted by Dr. Anton M. Jetten (Cell Biology Section, Laboratory of Respiratory Biology, National Institute of Environmental Health Sciences, National Institute of Health, USA)[27]. *Cbfβ2*$^{-/-}$ mice were gifted from Dr. Ichiro Taniuchi (RIKEN, Research Center for Allergy and Immunology, Kanagawa)[26]. *Rorγt*$^{gfp/gfp}$ mice were originally established by Dr. Dan R. Littman (Molecular Pathogenesis Program, Skirball institute of Biomolecular Medicine, New York University, USA) and purchased from The Jackson Laboratory (USA)[28]. *Id2*$^{-/-}$ mice were generated by the group of Dr. Peter Gruss[29]. All animal experiments were done with the approval of the Animal Research Committee of the Institute of Medical Science, The University of Tokyo.

1.2.2 *Examination of NALT formation*

Mice were sacrificed to obtain nasal tissues. Skin, maxilla, eyes, brain and other unnecessary parts of head were trimmed off. After briefly washed by ice cold PBS, remaining head part containing nasal tissue was fixed in 4%

paraformaldehyde at 4 degree Celsius for overnight. Next, tissue was subjected to fat-removal procedures; nasal tissue was dehydrated by sequential incubation in 70% EtOH, 80% EtOH and 90% EtOH each for at least 4 hours and then defatted in EtOH : Chloroform = 1 : 1 solution for 2 hours followed by hydrating incubations of 90% EtOH, 80% EtOH and 70% EtOH each for at least 2 hours. Whole this procedure should be done at 4 degree Celsius. After defatted, nasal tissue was decalcified by neutral EDTA solution which was made by dissolving 90 g EDTA· 2NA and 100 g EDTA· 4NA in 1 L pure water. Nasal tissue was packed in Tissue Tek (SAKURA) for rotation for more than 1 week at 4 degree Celsius in this decalcification solution. The solution was changed in the middle of this decalcifying period but, if not, nothing had changed in the result when the number of samples was small. After finishing the decalcification, the nasal tissue directly proceeded into dehydration for embedding. This process was automatically controlled by Auto-Kinetto (SAKURA-Finetek) with the program of 70% EtOH for 3 hours, 80% EtOH one hour, 90% EtOH 1 hour, 99% EtOH one hour, 100% EtOH (made from commercially available 99.5% EtOH supplied with molecular sieves) (I) 2 hours, 100% EtOH (II) 2 hours, 100% EtOH (III)

for 2 hours, Xylen (I) one hour, Xylen (II) one hour, Xylen (III) 2 hours, Paraffin (I) one hour and Paraffin (II) more than 2 hours. Tissue was transferred into paraffin pool of Dispensing Console IV (Sakura Tissue-Tek) and embedded in the paraffin. As is often the case with this embedding procedure, paraffin didn't fill the nasal cavity for many times. Paraffin infiltration into whole nasal cavity is necessary to strengthen the nasal septum and other architectures enough to bear the pressure of slicing. So the highest care should be taken to make sure that paraffin fills the nasal cavity. Paraffin block was coagulated on the ice. This block can be preserved for long time. Before slicing the tissue sections, the paraffin block should be well cooled on ice; this makes the block firmer and more suitable for section making. Sequential sections were transferred on the 42 degree Celsius water in water bath and separated into individual sections, and then selected sections were put on the slide glasses. These slide glasses were dried on 40 degree Celsius hot plate in order to fix the sections on the glasses. This incubation should not be shorter than 2 hours to avoid their peeling off from slide glasses during staining procedure. Next, tissue sections were subjected Hematoxylin - Eosin (HE) staining. HE staining was performed as follows:

Paraffin was removed by exposure to Xylen (I) for 3 min, Xylen (II) 1 min, Xylen (III) 1 min, 100% EtOH 1min, 99.5% EtOH 1 min, 90% EtOH 1 min, 80% EtOH 1 min, 70% EtOH 1 min, sections were washed by water for 10 min and then stained by Meyer's Hemotoxylin for 10 min followed by washing by water. Next, sections were stained by Eosin for 1 min. Sections were washed and dehydrated by water (I) for 3 sec, water (II) 3 sec, water (III) 3sec, 70% EtOH 10 sec, 80% EtOH 15 sec 90% EtOH 20 sec, 100% EtOH (I) 1 min, 100% EtOH (II) 1 min, 100% EtOH (III) 1 min, Xylen (I) 1 min, Xylen (II) 1 min, Xylen (III) 1 min. The stained section was embedded by 1 drop of Permount (Fisher Scientific) and covered with a cover glass (MATSUNAMI), and fixed by incubating at room temperature for at least one hour.

1.2.3 *RNA extraction and synthesis of cDNA*

Prepared cells were lysed by 1 ml of TRIzol reagent (invitrogen). Cells were not necessary washed by PBS. Lysate was pipetted vigorously until the syrupy materials were disappeared. In the most experiments, lysate with TRIzol were frozen to preserve at -80 degree Celsius. Frozen lysates were

thawed at 37 degree Celsius on block incubator for RNA extraction. 200 μl of chloroform were added into the tubes and mixed by vortex until the reagent became uniform pink-white color. After incubated at room temperature, tubes were centrifuged at 4 degree Celsius and max rpm for 5 min. This centrifugation separated the reagent into two layers; hydrophilic and hydrophobic layers. The upper layer, hydrophilic layer, was up to 550 - 600 μl, so 500 μl of it was transferred into a new tube. Aggregation which resides at interface between two layers should be excluded from the pipetted watery layer. One volume of isopropanol was added into the transferred sample and mixed vigorously by vortex. The tube was centrifuged at 4 degree Celsius and max rpm for 5 min. After centrifugation, the supernatant was carefully removed by pipette so as not to disorganize the pellet. The pellet was washed by 75% EtOH and dried up, and dissolved in RNase free water. The reverse transcription was performed by using 2 μg of RNA for template, if it was possible. When there were samples which could not provide such volume of RNA, all others were adjusted to the same concentration as it. The concentration of RNA template was adjusted to the same in order to exclude the possibility that the efficiency of the reverse transcription reaction is

affected by the amount of RNA template. 1 µl of Oligo dT primers and water were added to the sample up to 12 µl and mixed well. Sample was incubated at 70 degree Celsius on the block incubator for 10 min and then rapidly cooled on ice for 5 min. After flushing the water drops down, 4 µl First Strand Buffer, 2 µl 0.1 M DTT, 1 µl 10 mM dNTP and 1 µl Super Script III reverse transcriptase were added. Sample mixture was gently mixed by vortex and incubated at 42 degree Celsius for 1 hour. This incubation was performed in the air conditioning incubator to avoid water evaporation, which will change the salt concentration of reaction mixture, from sample. After finishing the cDNA synthesis, samples were incubated at 72 degree Celsius for 10min to inactivate the reverse transcriptase and then rapidly cooled on ice for 5 min. After flushing water drops, 1 µl (2 U) of RNase H was added, and the sample was mixed briefly and incubated at 37 degree Celsius on block incubator for 20 min. Following rapid cooling and flushing down completed the cDNA synthesis procedure.

1.2.4 *Quantitative PCR*

Quantitative polymerase chain reaction (qPCR) was performed by using 480

SYBR green (Roche). While it has the great advantage that it doesn't need specific probe for detection of amplified nucleotide sequences, it has the critical disadvantage of non-specific detection. To circumvent this problem, PCR products from primers for SYBR green amplification were subcloned and sequenced to confirm the specificity of PCR. When the manufacturer's data base couldn't provide the suitable set of primers and probes, the original primers were necessary to be designed. In creating primer sets for qPCR, forward and reverse primers were designed to flank intron(s) to avoid amplification of DNA derived from genome. PCR products from these original primers were also sequenced to check their PCR specificity. PCR reaction mix was made of 10 μl of SYBR green master, 3 μl water, 1 μl of 10 μM primers of forward and reverse and 1 μl of template which was 20× dilution of cDNA solution. PCR primers were shown below;

Gene		Sequence
P1Runx2	Fw	5'-cagcgcagtgacaccgtgtcagc-3'
	Rv	5'-gatgagcgacgtgagccc-3'
P2Runx2	Fw	5'-ggccacttcgctaacttgtgg-3'

	Rv	5'-ccggccatgacggtaacc-3'
Gapdh	Fw	5'-tgtccgtcgtggatctgac-3'
	Rv	5'-cctgcttcaccaccttcttg-3'

PCR program for amplification of Runx2 isoforms was;

For *P1Runx2* (short version) and *Gapdh*

<----------45 cycles---------->

Melting curve

95℃ 5min 95℃ 10sec 60℃ 10sec 72℃ 10sec

For *P1Runx2* (long version) and *P2Runx2*

<----------45 cycles---------->

Melting curve

95℃ 5min 95℃ 10sec 65℃ 10sec 72℃ 30sec

Selected amplification of target gene was confirmed by Tm calling and sequence analyses. The amounts of gene transcript of target genes were normalized by internal control gene *Gapdh*.

1.2.5 *Construction of expression vector*

Coding sequence of Runx2 isoforms were cloned from cDNA library prepared from murine cells. Primers used here were

Gene		Sequence
P1Runx2	Fw	5'-agatctatgcttcattcgcctcacaaacaaccac-3'
	Rv	5'-gtcgactcaatatggccgccaaacagactcatcc-3'
P2Runx2	Fw	5'-agatctatgcgtattcctgtagatccg-3'
	Rv	5'-gtcgactcaatatggccgccaaacagactcatcc-3'

PCR was performed with Phusion polymerase (FINZYME). PCR products were separated by agarose (invitrogen ultra pure agarose supplied with ethidium bromide from Nacalai) gel electrophoresis and the band of expected size was cut off on the UV exposition and collected in the 1.5 ml tube. Extraction of PCR product was done with Wizard gel and PCR clean up system (Promega). 300 μl of membrane bounding buffer (regardless of amount of gel, this volume was fixed) was added into 1.5 ml tube with cut off gel and incubated at 60 degree Celsius for 5 min. During incubation, tube was tapped for several times because mixing the buffer and gel promotes dissolution of gel. After the gel fragment was dissolved in the buffer completely, gel solution was transferred onto mini column and centrifuged at room temperature and max rpm for 1 min. After the flow through was

discarded, 500 μl of membrane wash buffer was added and centrifuged at the same settings. Membrane column was put on the new 1.5 ml tube and 30 μl of TE buffer was added onto membrane. The column and tube were centrifuged at most 14,000 rpm for 2 min. Because centrifugation of 1.5 ml tube with its rid open often breaks the tube (the rid will be tore off), the rpm should be much lower than max. Usually, the flow through yield will be lower than volume of added TE buffer, so the volume of TE must not be too small (no less than 20 μl). Because PCR product amplified by Phusion polymerase was blunt ended, it was ligated with pCR4-TOPO cloning vector (invitrogen) which is for blunt end product. 4.5 μl of PCR product, 1 μl of salt solution and 0.5 μl of pCR4-TOPO mix was mixed and incubated at room temperature for 5 min. Ligated vector was transformed into DH5α competent cells (TOYOBO), which were preserved at -80 degree Celsius in 20 μl aliquots. Frozen competent cells were thawed on ice, and 2 μl of ligated vector solution was added into it. The volume of vector added to competent cells should be lower than one-tenth of volume of competent cell solution. Cells were incubated for 20 min on ice, 30 sec at 42 degree Celsius and 2 min on ice. Then, 180 μl of SOC solution was added into cell solution, thus total volume

of cell solution would be 200 μl, and incubated at 37 degree Celsius with shaking. At the same time of the start of this incubation, LB-agar medium plate supplied with 50 μg/ml ampicillin was warmed under 37 degree Celsius in incubator with top side down to be dried to some extent suitable for seeding of cells. X-gal solution (100 mg X-gal in 5 ml dimethylformamide) was spread on the plate first, and cells in SOC solution were spread too. The plate was incubated in 37 degree Celsius for 16 hours. Too long incubation results in over growth of cell colonies and the appearance of "satellite colonies". After incubation, white colony were picked by a toothpick and dipped into 2 ml LB liquid medium supplied with 50 μg/ml of ampicillin. Blue colonies were made of cells possessing self-ligated pCR4 vector which encodes β-galactosidase. Culture plates with cell colonies can be stored at 4 degree Celsius for up to 1 month. 2 ml culture with liquid medium was incubated at 37 degree Celsius with shaking for 16 hours. After the culture period, culture medium was transferred into 2 ml tube and centrifuged at max rpm for 30 sec to pellet cells. Following plasmid extraction was done with Wizard plus SV minipreps (Promega). Supernatant was removed and 250 μl of cell suspension buffer was added. Pellet was loosened by vortex and

250 μl of cell lysis buffer was added. Tube was inverted for several times and 350 μl of neutralization buffer was added and mixed by inversion. Vortex in these steps should be avoided because it causes fragmentation of genome and contamination of it into plasmid sample. Neutralization was continued at 4 degree Celsius for 5 min. After the neutralization was completed, tube was centrifuged to pellet debris for max rpm for 10 min. The supernatant was transferred onto filter column and centrifuged at max rpm for 1 min. After removal of flow through, 700 μl of membrane wash buffer was added on the filter and centrifuged at max rpm for 1 min. Then, filter column was transferred on the new 1.5 ml tube and 100 μl of TE buffer was added for elution. Column was centrifuged for 2 min at adequate rpm (see above). Extracted plasmid was checked by restriction enzymatic digestion. pCR4 vector has two EcoRI recognition sites flanking insert region, so they were made use of to check the length of insert sequence when insert had no EcoRI recognition site. One selected vector, which had expected length of insert, was subjected to sequence analysis (Fasmac) and checked whole nucleotide sequence. After confirmation of DNA sequence, insert was cut out by scheduled restriction enzymes, whose recognition sites were prepared both

ends of insert. This enzymatic digestion was conducted in 50 ml mixture construction containing 27 μl of water, 15 μl of vector solution, 5 μl of 10× buffer, 1.5 μl of restriction enzymes × 2 (in case of double digestion). Digestion mixture was incubated at 37 degree Celsius for more than 1 hour and the fragment was purified by electrophoretic purification. After purification, fragment was ligated into expression vector. 4 μl of insert fragment, 1 μl of the enzymatic digested expression vector pFLAG-CMV6 (Sigma) and 5 μl of solution I (TaKaRa) were mixed on ice, and then incubated on block incubator at 16 degree Celsius for more than one hour. After ligation reaction, vector was transformed into DH5α which would undergo plate culture, liquid culture and plasmid extraction. The completed vector was also checked its accuracy by enzymatic digestion. Completed vector was transfected again into DH5α and plated to make a plate with single clone DH5α colinies. One of colonies was picked for 100 ml culture. Cells were collected and plasmid was purified by Nucleobond Xtra midi (TaKaRa). The extraction procedure followed manufacturer's instruction. Purified plasmid was dissolved in TE and the concentration was adjusted to 1 mg/ml. Completed plasmid was stored at -30 degree Celsius.

1.2.6 *Transfection of vector into animal cells*

Cells selected for the forced expression experiments were human embryonic kidney cell line immortalized by the expression of simian virus large T antigen; HEK293T. Transfection was performed by using lipofectamin 2000 (LF2000) (invitrogen). 293T cells at semi confluent density (approximately 2 $\times 10^6$ for 6 cm dish) were prepared in advance. 10 μl of LF2000 and 5-6 μg of expression vector were mixed in 1 ml of serum free culture medium at room temperature for 20 min. After incubation, 1.5 ml of serum free medium was added into LF2000-vector mixture. Culture medium was aspirated off from culture dish and 2.5 ml of LF2000-vector mixture was added into culture dish. This needed highest care so as not to let cells detach from the dish. 293T cells are the cells which detach from dish so easily. Cells were incubated at 37 degree Celsius for 4 hours in the CO_2 incubator. During this incubation period, culture medium with 20% FCS was prepared and warmed to 37 degree Celsius in the water bath. 2.5 ml of this culture medium with 20% FCS was added to the cell culture at the last of incubation. Cells were cultured for more one or two days until harvesting.

1.2.7 *Preparation of cell lysate for immunoprecipitation and western blotting*

Cells were harvested by trypsinization and washed by cold PBS at least twice to remove remaining proteins, for instance ones derived from FCS. Washed cells were transferred into 1.5 ml tube and lysed with 0.5% Nonided P-40 in 20 mM Tris (pH 7.5) and 150 mM NaCl. Cells suspended in lysis buffer were rotated at 4 degree Celsius for 1 hour and then centrifuged at 4 degree Celsius, max rpm for 10 min to pellet undissolved cell membrane and cell components. Supernatant was collected as lysate sample and preserved, if it was needed, at -80 degree Celsius. Immunoprecipitation was performed with protein G - sepharose gel. First, non-specifically binding materials to sepharose were removed by adding 20 - 50 μl of sepharose beads and incubation at 4 degree Celsius for 1 hour with gentle rotation. Pipetting of this sepharose beads should be done with tips whose tips were cut off otherwise the tips would be blocked by bead particles. After incubation, tube was centrifuged at 4 degree Celsius, 3000 rpm for 2 min and supernatant was transferred into a new tube. 1 μl (up to 5 μl as maximum) of antibody solution was added into lysate and the sample was incubated at 4 degree Celsius with gentle rotation for 1 hour or overnight. Then 20 - 35 ml of

protein G - sepharose beads were added into tube followed by rotation at 4 degree Celsius for 1 hour. After centrifugation at 4 degree Celsius 3000 rpm for 2min, supernatant was aspirated off and beads were washed by 1 ml of lysis buffer for 3 - 6 times. Then these beads could be used as immunoprecipitated sample. One volume of sample buffer was added into beads or, when cell lysate was used, 10 μl of lysate sample was mixed with 5 μl of 3×sample buffer, and they were boiled at 100 degree Celsius on the block incubator for 10 min. After incubation, the sample was cooled at room temperature. This cooling down should be done at room temperature because SDS would crystalize if it was cooled on ice. Gels which were used for electrophoresis were SuperSep Ace gradient gel (Wako). Sample was loaded on the gel and migrated at 20 V for 20 min at first. Because SuperSep gel doesn't have stacking area, sample should be stacked under this starting voltage. Then, voltage was changed to 40 V for separation for 40 min. Before finishing the electrophoresis, membrane was activated by being soaked in methanol for a few minutes and transferred into transfer buffer (Tobin Buffer). Proteins on the gel were transferred onto membrane in submarine type transferring apparatus at 4 degree for 1 hour. After transfer, membrane

was incubated in the blocking buffer (5% skim milk in TBST) for 30 min at room temperature or for overnight at 4 degree Celsius. After briefly washing out the skim milk by TBST, the membrane was incubated with primary antibody. Four different anti-Runx2 antibody were tested; clone rabbit polyclonal M-70 (Santa Cruz), mouse monoclonal 2B9 (Abnova), mouse monoclonal ascites 4E5 (Abnova), mouse monoclonal 8G5 (MBL). All antibodies were tested ×1000 dilution as first antibody combined with × 3000 diluted secondary antibodies (anti-rabbit IgG or anti-mouse IgG purchased from Santa Cruz). For antibody reaction, membrane was incubated on 1.5 ml of filtrated TBST mixed with designated antibodies on Parafilm (Pechiney Plastic Packaging Company) for 1 hour at room temperature or for overnight at 4 degree Celsius. Membrane was washed by TBST with gentle shaking for three times each for 10 min. Excessive wash buffer on the membrane was removed and it was brightened by Western Lightning (Perkin Elmer) and the signal was detected by Amersham Hyperfilm ECL (GE Healthcare) exposed in manual X-ray film cassette (OKAMOTO manufacturing). Film was developed by FPM 800A (Fujifilm) with reagents RD-1B (Fujifilm). In some experiments, the anti-Runx2

antibodies were labeled by Horse Radish Peroxidase (HRP) by Peroxidase Labeling kit-NH_2 (DOJINDO). The experimental procedure followed manufacturer's instruction. These labeled anti-Runx2 antibodies were used at $\times$2000 dilution.

1.3 Results

1.3.1 *Generation of mouse finished successfully but that line showed neonatal lethality*

As described in my dissertation for Master Degree, I constructed targeting vector for P2Runx2 knockout mouse and transfected it into ES cell line, and then obtained recombined cell lines (Figure1). One of them successfully generated chimera mouse which gave rise to birth of heterozygous gene manipulated descendants. However, these heterozygotes didn't generate homozygous mice until the number of genotyped mice summed up to 100 (wild type 44, hetero 68, homo 0). There were constantly observed dead pups in the group of newborns. This fact drove me to examine the genotypes of them. I found that most of dead neonates were homozygotes. The precise homologous recombination was confirmed by southern blot (Figure2 A,B) and sequence analysis of point mutation introduced into first ATG of *P2Runx2* (Figure2 C).

At the same time, I prepared CAG-Cre mice, which possess Cre recombinase transgene under the artificial CAG promoter and express it in their whole body, in order to delete neomycin resistant gene cassette (*neo*^{r})

because I wished to exclude the possibility that *neo*^{r} compromises gene expression of Runx2 or others. I picked mice without Cre after intercrossing two lines of mouse, *neo*^{r} possessing *P2Runx2* manipulated one and CAG Cre transgenic one, since this CAG transgenic mouse has some minor disorder for survival. When *neo*^{r} was deleted, the homozygote mice could grow up to be adults and showed no sign of growth defect (wild type 27, hetero 49, homo 27). I confirmed *neo*^{r} deletion by gene sequence at the site of *neo*^{r} insertion and southern blot analysis (Figure3 A, B and C). The results showed that *neo*^{r} removal was occurred successfully and there remains nucleotide sequence derived from loxP after Cre-loxP elimination of DNA sequence (Figure3 B). At first, I did genotyping of newly established *neo*^{r} depleted mice with primers designed so as to flank remnant of loxP. I expected to distinguish PCR product by the size of bands, but it was difficult because, although heterozygote result showed two bands of different size, the position of band from wild type mice (bands of wild type allele) and mutated mice (from mutated allele) were almost same. I don't know, however, why this phenomenon occurred. To establish more suitable genotyping system for these mice, I decided to make use of 5' deletion region of targeting vector

(Figure4 A). By conducting PCR by primers flanking this region, wild type allele was supposed to produce approximately 800bp fragment and mutated allele was supposed to produce 300bp fragment. But the mice of each genotype, which was determined by former genotyping system, showed same size of bands. This result suggested two possibilities; (i) experiment didn't work well due to some trouble such as poorly designed primers (ii) experiment worked well but mutated allele didn't have deleted region. To address this question, I did same PCR with template genomic DNA of ES cells and original targeting vector which I confirmed had sequence deletion. The result clearly showed that ES cell line #11, which was only successfully incorporated into blastocyst and germ line transmitted, had experienced incomplete recombination of targeting vector (Figure4 B). In spite of my intensive trials, other ES cell lines and newly prepared additional three ES cell clones with homologous recombination of targeting vector (of course they have 5' deletion) could never generate germ line transmitted chimera mouse. Consequently, I designed a sense primer whose 3' end was located on the remnant of loxP and managed to obtain reasonable genotyping results. And I modified description of gene mutated mice (Figure4 C). The varied results by

neo^r deletion implied that the insertion of *neo*^{r} into intron after the first exon of *P2Runx2* was the cause of lethality of homozygote mice with *neo*^{r} cassette. So I would like to call *neo*^{r}-possessing homozygous mice as *P2Runx2*$^{neo/neo}$ and whole body *neo*^{r}-depleted mice as *P2Runx2*$^{mut/mut}$ mice (still conveying ATG => TGA point mutation) hereafter. Since *P2Runx2*$^{mut/mut}$ mice have point mutation on their translation start codon of *P2Runx2*, P2Runx2 protein can not be produced theoretically. But they didn't show any problem on their survivals apparently. This result implies that the translation starts from second methionine, which located at 25th amino acid in the first exon of *P2Runx2*, and that truncated P2Runx2 works as well as full length Runx2, suggesting P2Runx2 specific amino acid sequence (MRIPV) is indispensable for its function. The confirmation of the expression of truncated P2Runx2 needs western blot analysis.

I examined NALT formation of *P2Runx2*$^{mut/mut}$ mouse and found it comparable to wild type (Figure4 D). This result was reasonable and within expectation because *P2Runx2*$^{mut/mut}$ mouse doesn't show any phenotypes which could be related to decreased P2Runx2 expression. Thus Runx2 function of *P2Runx2*$^{mut/mut}$ mouse was supposed to be equivalent to that of

wild type. To clarify the role of P2Runx2 to the NALT formation, it was necessary to get the adult (at least no younger than 10 day old) P2Runx2 diminished mice.

1.3.2 *Characterization of generated mouse line by gene and protein expression*

After generation of gene manipulated mouse, I was keen to confirm the disruption of *P2Runx2* expression by means of reverse transcription followed by quantitative RT-PCR and western blot analysis. These analyses should show the expected disappearance of *P2Runx2* and intact *P1Runx2* expression. In order to examine *P1Runx2*, which is expressed only in bone tissue, I utilized fetal carvarial cell to examine gene expression.

For examination of gene expression, I prepared calvarial cells from enzymatically digested calvaria. To avoid the contamination of undesired cells, *e.g.* from skin or brain, I discarded first fraction of sequential digestions and pooled later fractions. RNA extracted by general TRIzol method were reverse transcribed with oligo dT primer to obtain full length cDNA for examination because I had several check points other than simple

gene expression. Our quantitative PCR (qPCR) machine was purchased from Roche and the company provide universal probe library for which primer sets for PCR amplification can be automatically designed to adjust certain universal probes. I designed, however, primers for my assays by myself because Roche's web program couldn't return primer sets which can distinguish P1 and P2 isoforms of *Runx2*. When I made primers for qPCR, I took great note of the length of its amplicon, melting temperature (Tm) and containing of intron between two primer annealing exons (Figure5 A). I did qPCR with SYBR green whose detection specificity is less accurate than universal probe method, so I confirmed the nucleotide sequence of amplified cDNA by gene sequence. The result of qPCR exhibited significant decrement of *P2Runx2* transcripts to the extent of one-tenth of wild type littermate controls (Figure5 B). Despite this decreased transcripts of *P2Runx2*, the amount of *P1Runx2* was not changed significantly and seemed, except for slight decrement of it, to be intact (Figure5 B). Abrogation of *P2Runx2* expression resulted in the significant decrement of total *Runx2* expression which was examined primer sets for the common region of P1 and P2 *Runx2* (Figure5 B). These results suggested that the established mouse has

diminished *P2Runx2* expression in homozygote and the insufficiency of *P2Runx2* might lead the lethality of this mouse.

To further confirm the decreased Runx2 expression in terms of protein production, I purchased some clones of antibodies and check their efficiency. For positive control of this experiment, I cloned cDNA of both P1 and P2Runx2, and constructed FLAG-tagged expression vectors of them. In the course of this gene cloning, I found some less examined splicing variants, among them was the one which lacks exon6, as previously reported (cf. Figure1)[30]. I decided to make use of the cDNA containing exon6, as "full length" for this experiment. First, I transfected this expression vector into HEK293T cell line to check the completed construction of the vector. I did immunoprecipitation by using anti-FLAG antibody and blotted the membrane by the same clone of anti-FLAG antibody. This result would be the reference for the following antibody screening. Using this transfectant, I blotted the membrane with different three antibodies and obtained the result showing the same size of band as FLAG-I.P. FLAG-I.B. band from two of them. Next, I tested the efficiency for I.P. of these antibodies by anti-Runx2-I.P. and anti-FLAG-I.B., and found two of them can be used for

I.P. But in combination of these antibodies for I.P. and I.B., in other words, experiments devoid of anti-FLAG antibody, which would be necessary to examine endogenous protein levels of mouse cells, couldn't work well partly because the affinity and specificity of these antibodies were not enough for combined I.P. and I.B. I purchased one more antibody from MBL and labeled it with Horse Radish Peroxidase (HRP). The experiments with this antibody exhibited two bands that were reported previous study and explained as signal of P1 and P2Runx2 in the article[31], but the size of band was different compared to recombinant protein (Figure6 B). Again, although this antibody from MLB was most efficient among tested, it was not sensitive enough to detect the endogenous protein even lysate from MC3T3 cells which express high amount of both types of Runx2 (cf. Figure6 A). These results suggested that it is too difficult to obtain data clear and convincing enough for publishing from protein experiments.

Further Characterization of P2Runx2$^{neo/neo}$ mice

Previous reports showed that the intronic insertion of *neo^r* resulted in the generation of target gene-neo^r fusion transcript[32-35]. The lethality of

P2Runx2$^{neo/neo}$ mice was clearly controlled by the existence of *neo*^{r}, implying that *neo*^{r} interferes correct splicing of *P2Runx2*. To address this possibility, I conducted PCR amplification by using primers flanking the intron in which *neo*^{r} was inserted (e.g. PCR with primers 2 and 6 of Figure7 A). Despite the intensive trials, I couldn't obtain longer PCR products of *Runx2* which contain nucleotides derived from *neo*^{r}. Therefore, in contrast to some of previous reports, *P2Runx2*$^{neo/neo}$ mice apparently do not have fusion transcripts which include internalized fragment of *neo*^{r} in *Runx2*. Next, I tested the possibility that the mRNA synthesis is interrupted in the consequence of the aberrant splicing. I conducted PCR amplification by using primers, one is on Runx2 and the other is on *neo*^{r} (Figure7 A). The primers on *Runx2* were designed on both P1 and P2 specific region. PCR conducted by each primer efficiently amplified mRNA sequences, suggesting the existence of *Runx2-neo*^{r} fusion transcripts induced by P1 and P2 promoters (Figure7 B). The PCR product was subcloned for gene sequence analysis. The directly connected *Runx2-neo*^{r} sequence was confirmed (Figure7 C top). I also tested PCR with primers on *neo*^{r} and Runx2 exon4, and found the 5' end of *neo*^{r} (note: *neo*^{r} was reverse oriented in this construction) and Runx2 exon4 were

also combined directly. This PCR product was also subcloned for sequence and the junction was determined (Figure7 C bottom). Of note, it is reasonable to think there exist at least different two splicing patterns. From the result in Figure5 B, it can be assumed that *Runx2-neo*^{r} type transcript reaches the site of primer 4 at least (Figure7 D pattern A). Contrary, *neo*^{r}*-Runx2* type transcript is spliced before the site of primer4, suggesting that this is different transcript from pattern A (Figure7 D pattern B). Although it is possible that there are other types of transcripts generated, these aberrant splicing does not make *Runx2-neo*^{r}*-Runx2* type transcript. Therefore, all of transcriptions stop in *neo*^{r} or start in *neo*^{r} irregularly.

From the results described above, the suspicion about the accuracy of qPCR appeared. PCR primers for *P1Runx2* illustrated in Figure5 A don't flank intron between exon3 and 4, where *neo*^{r} resides. Considering the newly unveiled transcription interrupting mechanism of *neo*^{r}, the primers should be designed to flank that intron. Therefore, I modified the primer settings as shown in Figure8 A and conducted gene quantification again. The result strikingly showed that *P1Runx2* was also decreased significantly (Figure8 B). It is true that the data shown in Fugure5 was correct and reliable, but the

setting of primers was not adequate for *P2Runx2*$^{neo/neo}$ mouse. In conclusion, *P2Runx2*$^{neo/neo}$ mice are not P2Runx2 specific knockout mice but both P1 and P2 isoforms diminished ones. In spite of non-specific abrogation of *Runx2* gene, tissue specifically restricted expression pattern of its isoforms enable me to say *P2Runx2*$^{neo/neo}$ mouse is *P2Runx2* specific knockout mouse model in terms of lymphoid tissue organogenesis.

1.3.3 *Rescue of lethality of P2Runx2*$^{neo/neo}$ *mice by site specific neo*^{r} *deletion*

Since NALT formation starts one week after birth, neonatal lethality of *P2Runx2*$^{neo/neo}$ mice was obstacle which must be removed to examine NALT development of these mice. I obtained Col2a1-Cre transgenic mouse, which expresses Cre recombinase under the control of chondrocyte specific Col2a1 promoter, so as to solve the problem by intercrossing *P2Runx2*$^{neo/neo}$ mice with this mouse. Although most suspected phenotype of *P2Runx2*$^{neo/neo}$ mice was defect of bone formation, I used the chondrocyte specific Cre transgenic strain because it was the only available Cre transgenic mice related to bone tissue at that time. So I made use of this mouse to excise neo^{r} cassette in the bone-related tissue, while it would let other tissues still

possess neo^r. This purpose was successfully achieved because, among Cre expressing mice, half of homozygote mice survived as healthily as wild or heterozygote mice (wild type 17, hetero 31, homo 8 among Cre^+ mice). These mice showed no weakness of appearance, they are at the same size as their littermate controls, and they do not have any other physical disorders. I confirmed the existence of neo^r cassette in these mice by performing southern blot analysis with genome extracted from their tails (Figure9 A). Next, I testified whether the P2Runx2 decrement is maintained by examining the gene expression of splenocytes of these mice and confirmed that it was still at the low level (Figure9 B). Given that these Col2a1-Cre/*P2Runx2*$^{neo/neo}$ mice have diminished *P2Runx2* expression in all tissues and cells except for bone related ones, *P2Runx2* expression in NALTi of these mice also decreased. So I examined the NALT development of Col2a1-Cre/*P2Runx2*$^{neo/neo}$ mice, however, I found these mice have mature NALT structures in their nasal cavities (Figure9 C).

Runx family proteins share highly conserved RUNT homology domain (RHD) and a report suggested the functional redundancy of these family proteins[8]. P2Runx2 is expressed in whole body and

Col2a1-Cre/*P2Runx2*$^{neo/neo}$ mice have reduced *Runx2* gene expression other than bone related tissues, so I expected some phenotypes would be observed in these mice. First, I examined the Treg cell population of these mice because Runx1 and Cbfβ work together to induce and maintain the expression of transcription factor Foxp3[10-12]. I examined in vivo Treg cell frequency in tissues such as spleen and intestine, and the efficiency of naïve T cell to give rise to Treg population after in vitro stimulation. I didn't find any differences of Treg between Col2a1-Cre/*P2Runx2*$^{neo/neo}$ mice (Figure9 C). Next, I tested the possibility that IL-17 producing T cell (Th17) cell population because the relationship of Runx1 to RORγt were reported[36]. They also showed Runx2 also binds to RORγt demonstrated by the co-immunoprecipitation assay. I prepared small intestinal lymphocytes which contain a number of Th17 cells in steady state and compared Th17 cell population between wild type and Col2a1-Cre/*P2Runx2*$^{neo/neo}$ mice, but found no difference (Figure9 D). Cbfβ knockout mice shows severe defect in development of TCRγδ T cells[25], so I checked the possibility whether the cooperator of Cbfβ in maturation of this cell subsets is Runx2, but the hypothesis was denied (Figure9 D). Finally, I checked the IgA-producing cell

population in small intestine because, according to the previous study, Runx2 regulates B cell class switch recombination together with Runx3[17]. When a mouse is doubly deficient in Runx2 and Runx3, IgA^+ plasma cell number will dramatically fall down. Of course, such a double deficient mouse is lethal, so they did fetal liver adaptive transfer to examine this issue, and mentioned that single knockout mice of each gene didn't show phenotype (Figure9 D). According to their observation, it was not hopeful to test this issue in Col2a1-Cre/*P2Runx2*$^{neo/neo}$ mice and I didn't find any difference in IgA producing cell population of wild type and mutated mice. From these results, P2Runx2 is little, if any, responsible for immune regulation. But, to make conclusion, there exists one problem that although Col2a1-Cre/*P2Runx2*$^{neo/neo}$ mice significantly diminished expression of P2Runx2, detectable amount of gene transcripts were observed in these mice. So, conditional complete deletion model of Runx2 is necessary for more accurate examination of role of P2Runx2 in immune cells.

1.3.4 *Poor reproducibility of previous results*

Along with examination described above, I tested the reproducibility of

previous results. First, I examined Cbfβ2 deficient mice which became one of the strongest evidences showing involvement of P2Runx2 to NALT formation. Many of tissue sections of Cbfβ2 knockout mice had NALT structures regardless of their genetic background (C57BL/6, Balb/c or 129sv/C57BL-mixed) and difference of fostered facility (IMSUT SPF, conventional room or RCAI) (Figure10 A). Actually, in many cases, the size of NALT in Cbfβ2 deficient mice seemed smaller than that of wild type, though I didn't measure them. Therefore it might be possible that these mice have some difficulties in development of NALT, but I can not say that these mice "lack" NALT structure.

In addition, I tried to clarify the Id2, the master regulator of LTi cell development, deficient mice, whose NALT structure was reported to disappear completely[7]. This mouse strain has tendency to less reproductive when it is backcrossed into a specific genetic background other than 129/Sv, I used mouse of background of C57BL/6J and 129/Sv mixed. It was true that NALT formation of Id2 deficient mice was severely impaired, but I found the obvious lymphoid aggregation at the site of NALT, the bottom of nasal cavities (Figure10 B). Although, in the previous report, the authors

distinguished phenotype of Id2 deficient mice from other NALT malformation phenotypes, such as LTα or IL-7R deficient mice, my result of Id2 deficient mice has nothing enough to classify it into different group from those of other gene knockout mice rationally. Moreover, they did identification of NALTi by utilizing the Id2 knockout mice as "complete NALT-deficient mice" and showed that NALT deficiency was overcome by adaptive transfer of wild type LTi fraction. But, considering my result of Id2 NALT formation, I cannot exclude the possibility that their observation of "rescued NALT formation" was just the looking at the NALT-like structure formed at the site regardless of the "NALTi" inoculation. Taken these results and consideration together, there remain no reasons theoretically to continue this NALTi based project any more. This was why I quit this research.

What is more, I got some results which are incompatible with previous reports. Transcription factor RORγ was reported to be crucial for lymphoid organogenesis[1,4] but not to be involved in NALT formation[6]. It is true that among *Rorc*$^{-/-}$ mice, I found one which had well developed NALT structure, but other two mice showed diminished NALT formation (Figure11 A). And *Rorγt*$^{-/-}$ mice, lacking RORγ in the isoform specific way, showed also

minimalized NALT structures (Figure11 C). Although I have not reached the reason of this inconsistence, the background theory, which tells that NALT formation is completely independent of RORγ transcription factor, must be revised radically. And I found Mesenteric Lymph Node (MLN)-like lymphoid structures in the mesentery of *Rorc*$^{-/-}$ mice, which should not have such structures (Figure11 B). This observation was very preliminary, but it implies the necessity to review drastically the current understanding of lymphoid tissue organogenesis. Of course, this structure could be the Fat-Associated Lymphoid Cluster (FALC)[37]. Further examination of cell population will reveal which classification is adequate to these unexpected lymphoid structures.

1.4 Discussion

Generation of P2Runx2 manipulated mouse was performed by using mouse ES cell line derived from 129/Sv background. Total six targeting vector recombinated ES cell clones were injected into mouse blastocyst; among them was clone #11 which could give rise to germ line transmitted chimera mice. In this ES cell line #11, targeting vector recombination was incomplete so that 5' long arm deletion sequence was not incorporated into genome. Although several trials were carried out, other ES cell lines which possess successfully incorporated targeting vector were not transmitted into germ line of chimeric mice. The reason of this failure was unknown, but I found a group reporting that the generation of P2Runx2 specific knockout mice is difficult because of the low efficiency of vector recombination into targeted region[31] (presumably the same region as our target). In fact, I did obtain accurately recombinated ES cell lines. I can not make conclusion yet, but there may be some important elements for mouse embryonic development in the 5' upstream region of the first exon of *P2Runx2*.

P2Runx2$^{neo/neo}$ mice died soon after birth, which is phenocopy of Runx2-null mice. This result drove me to examine *Runx2* gene expression in

their calvarial cells. For quantification of *Runx2* in the isoform specific way, I designed primers by myself because the Roche website (https://www.roche-applied-science.com/sis/rtpcr/upl/index.jsp?id=UP030000) did not provide primers which can distinguish *Runx2* isoforms. When I designed primers, I followed mainly two principles; 1) The length of amplicon should be 100 bp approximately 2) Primers should flank at least one intron. (1) is critical for effective amplification by DNA polymerase of SYBR green system. (2) is necessary to avoid undesired detection of genome, which I think can not be removed completely by conventional RNA purification procedure even though DNase was used. In case of PCR for *Runx2* isoforms, one of the primers should be located on the isoform specific region, and this greatly limited the flexibility of design. I set primers for *P1Runx2* on exon2 and 3. For *P2Runx2*, I set primers on exon3 and 4 because of the position of intron. Such difference of primer design later resulted in the fatal misunderstanding of *Runx2* expression profiles of $P2Runx2^{neo/neo}$ mouse. In this experiment, I got results that *P2Runx2* was decreased, despite the expression of *P1Runx2* was not changed.

$P2Runx2^{neo/neo}$ mice can survive when neo^r cassette is removed by

Cre-loxP system. This result implies that the existence of *neo*^{r} compromises the gene expression of *P2Runx2*. There are some reports showing that insertion of *neo*^{r} cassette into the intronic region of a gene resulted in the generation of combined mRNA of the targeted gene and *neo*^{r} transgene[32-35]. Targeting construct and the phenotype of *P2Runx2*$^{neo/neo}$ mice is so similar to the reported gene manipulated mice that I checked the production of *Runx2-neo*^{r} fusion transcript in *P2Runx2*$^{neo/neo}$ mice. Although full length *Runx2* in which *neo*^{r} transgene gene was inserted was not detected, I found two types of *Runx2-neo*^{r} fusion transcripts. It might be strange that although exon3-*neo*^{r} fusion and *neo*^{r}-exon4 fusion were observed, I could not detect exon3-neo^{r}-exon4 double fusion transcript. But this is true result and one of the major reasons why I had not realized the generation of these fusion transcripts at first step of gene expression profiling. Splicing seems to occur under the unknown, but particular rules, since the only single product was generated by PCR amplification. Although exon3-*neo*^{r} fusion product even does not follow AG-GT rule, there may be the hidden mechanism for this irregular splicing. These fusion RNAs were equally amplified regardless of which Runx2 isoforms the primer specifically attaches, suggesting the

transcription of both P1 and P2 isoforms were interfered by *neo*^{r} to the same extent. To test this possibility, I conducted quantitative PCR for *P1Runx2* again with modified primer set which placed exon2 and 4. To my regret, my speculation was revealed to be right. *P1Runx2* expression in *P2Runx2*$^{neo/neo}$ mouse was also decreased significantly compared to wild type. The amount of gene transcript was one-third of wild type, while *P2Runx2* was decreased to one-tenth of wild type. From this result, it can be said that *P2Runx2* is more susceptible to transcription interference by *neo*^{r} presumably due to the transcription start site of it is closer to *neo*^{r} cassette, whose PGK promoter powerfully recruits transcriptional protein complex and might compete with P2 promoter of *Runx2*, than P1 counterpart. I modify the description of *P2Runx2*$^{neo/neo}$ mouse; it does not lack *P2Runx2* specifically, but both isoforms of Runx2 are significantly diminished. Fortunately, since the expression of *P1Runx2* is strictly restricted within ossified tissues, this mouse model can be used as *P2Runx2* specific modified model for NALT organogenesis.

Surprisingly, the fatal effect of *neo*^{r} insertion was rescued by the removal of it in the chondrocyte specific way. The lethality of Runx2-null

mice was reported to be due to the failure of breathing[13]. If that observation (this was not the experimental result, but just an observation), in addition to result from this study, is true, one can say that the crucial skeletal part for breathing is made of cartilage. This notion is consistent with the report showing that lethality of Runx2-null mice was rescued by ectopically expressed *Runx2* transgene under the control of Col2a1 promoter[38]. This result supports the idea that Runx2 is also crucial for the chondrogenesis[39,40].

P2Runx2$^{mut/mut}$ mice have point mutation on their translation start codon into STOP codon but, nevertheless, they were completely rescued from their lethality. According to dose-dependent hypothesis (see Part2), these healthy mice should have sufficient amount of Runx2 protein. The second methionine is located as 25th amino acid at *P2Runx2* exon1. Considering my observation, *P2Runx2*$^{mut/mut}$ mice seem to express truncated form of P2Runx2, which lacks specific sequence for P2 isoform (5 amino acids; MRIPV), and it works efficient enough to induce osteogenic gene expression. This means that the start sequence MRIPV is not indispensable for the function of P2Runx2, further suggesting that Runx2 isoforms don't have

distinctive roles accomplished by their specific N-terminal amino acid sequences. Actually, although it is necessary to confirm the existence of truncated form of protein, I could not establish the western blot detection system for endogenous protein, it remains to be confirmed by more efficient antibody.

In this study, I found that all of the gene manipulated mice examined, including "NALT-deficient" Id2 knockout mice and Cbfβ2 deficient mice which provided fundamental data to this study, had NALT or NALT-like structure. The data from Id2-deficient mice is fatally negative for this study because NALTi was defined by adaptive cell transfer experiment into Id2-deficient mice. Given that intact Id2-deficient mice have NALT-like cell aggregation, how can we distinguish the original NALT from newly generated NALT by the effect of wild type "NALTi"? I would like to suggest the possibility that the NALT structure observed in previous report could be seen regardless of "NALTi" inoculation. Cbfβ2 deficient mice had much more developed NALT structure than *Id2*$^{-/-}$ mice as far as I examined. So my interest is why my predecessors took these mice as NALT-deficient ones. During series of my experiments about NALT, I found that the size of NALT

is different from mouse to mouse even though they are on the same genetic background. Even a NALT of wild type mouse could be found half the size of another wild type mouse. This feature can mislead the researchers who determine existence of NALT by simple observation of nasal tissue sections. In order to further confirm the absence of NALT, the previous report showed PNAd (Peripheral Node Addressin) staining pattern in addition to HE staining[7]. But is it suitable for the examination of lymphoid tissue? Isn't it the matter of course that an ill developed lymph node has ill developed HEVs (High Endothelial Venules)? I wonder what kind of model they had imaged at that time; which comes first, HEV or lymph node. Although they denied the involvement of commensal flora by examining the germ-free mice which have comparable NALT structure to bacteria sufficient mouse, I still think some environmental factor, such as bacteria or food, can affect the development of NALT. Even if fostered in the same room, the commensal flora of a mouse is different in family to family (results of my preliminary trials). This diversity of bacteria might result in the different levels of NALT development of mice reared in the same facility. The problems appeared here provide an important lesson that when one says "something does not exist",

he should further make sure that it is not just observable. Quantitative examination is preferable in biology, where anyone can not declare “a certain thing does not exist”, instead, he will just say “it is not detected”. Predecessors should have discussed NALT size, not existence.

Because the P2Runx2 expression level is kept low in Col2a1-Cre/*P2Runx2*$^{neo/neo}$ mice except for in cartilage, I briefly tested the possibility that the decreased expression of Runx2 causes the immunological dysfunction. Although there are not powerful evidences showing the roles of Runx2 in immune cells, the fact that Runx transcription factor family members recognize DNA motif by their conserved RUNT domain implies that Runx2, besides Runx1 and Runx3, has roles in immune regulation. To address this possibility, I tested the immune cells of Col2a1-Cre/*P2Runx2*$^{neo/neo}$ mice for already published subjects as functions of Runx1 or Runx3. Contrary to my expectation, I did not observe any difference between Col2a1-Cre/*P2Runx2*$^{neo/neo}$ mice and Col2a1-Cre/*P2Runx2*$^{+/+}$ mice. This result can be interpreted in 3 ways; 1) Runx2 has no roles in immune regulation. 2) All Runx family transcription factors work in redundant way which masks the effect of diminishing Runx2

expression. 3) Because Col2a1-Cre/*P2Runx2*^{neoneo} mice express trace amount of P2Runx2, this Runx2 works well enough to maintain immune cell functions. To make conclusion about this issue, mouse completely lacking Runx2, by conditional deletion of Runx2 hopefully, is needed.

1.5 References

1 Kiyono, H. & Fukuyama, S. NALT- versus Peyer's-patch-mediated mucosal immunity. *Nat Rev Immunol* 4, 699-710 (2004).

2 Csencsits, K. L., Jutila, M. A. & Pascual, D. W. Nasal-associated lymphoid tissue: phenotypic and functional evidence for the primary role of peripheral node addressin in naive lymphocyte adhesion to high endothelial venules in a mucosal site. *J Immunol* 163, 1382-1389 (1999).

3 Fagarasan, S. & Honjo, T. Intestinal IgA synthesis: regulation of front-line body defences. *Nat Rev Immunol* 3, 63-72 (2003).

4 Mebius, R. E. Organogenesis of lymphoid tissues. *Nat Rev Immunol* 3, 292-303 (2003).

5 Benezech, C. *et al.* Lymphotoxin-beta Receptor Signaling through NF-kappaB2-RelB Pathway Reprograms Adipocyte Precursors as Lymph Node Stromal Cells. *Immunity* 37, 721-734 (2012).

6 Harmsen, A. *et al.* Cutting edge: organogenesis of nasal-associated lymphoid tissue (NALT) occurs independently of lymphotoxin-alpha (LT alpha) and retinoic acid receptor-related orphan receptor-gamma, but the organization of NALT is LT alpha dependent. *J Immunol* 168, 986-990 (2002).

7 Fukuyama, S. *et al.* Initiation of NALT organogenesis is independent of the IL-7R, LTbetaR, and NIK signaling pathways but requires the Id2 gene and CD3(-)CD4(+)CD45(+) cells. *Immunity* 17, 31-40 (2002).

8 Blyth, K., Cameron, E. R. & Neil, J. C. The RUNX genes: gain or loss of function in cancer. *Nat Rev Cancer* 5, 376-387 (2005).

9 Chen, M. J., Yokomizo, T., Zeigler, B. M., Dzierzak, E. & Speck, N. A. Runx1 is required for the endothelial to haematopoietic cell transition but not thereafter. *Nature* 457, 887-891 (2009).

10 Ono, M. *et al.* Foxp3 controls regulatory T-cell function by interacting with AML1/Runx1. *Nature* 446, 685-689 (2007).

11 Kitoh, A. *et al.* Indispensable role of the Runx1-Cbfbeta transcription complex for in vivo-suppressive function of FoxP3+ regulatory T cells. *Immunity* 31, 609-620 (2009).

12 Rudra, D. *et al.* Runx-CBFbeta complexes control expression of the transcription factor Foxp3 in regulatory T cells. *Nat Immunol* 10,

1170-1177 (2009).

13 Otto, F. *et al.* Cbfa1, a candidate gene for cleidocranial dysplasia syndrome, is essential for osteoblast differentiation and bone development. *Cell* 89, 765-771 (1997).

14 Komori, T. *et al.* Targeted disruption of Cbfa1 results in a complete lack of bone formation owing to maturational arrest of osteoblasts. *Cell* 89, 755-764 (1997).

15 Mundlos, S. *et al.* Mutations involving the transcription factor CBFA1 cause cleidocranial dysplasia. *Cell* 89, 773-779 (1997).

16 Jeong, J. H. *et al.* Expression of Runx2 transcription factor in non-skeletal tissues, sperm and brain. *J Cell Physiol* 217, 511-517 (2008).

17 Watanabe, K. *et al.* Requirement for Runx proteins in IgA class switching acting downstream of TGF-beta 1 and retinoic acid signaling. *J Immunol* 184, 2785-2792 (2010).

18 Stock, M. & Otto, F. Control of RUNX2 isoform expression: the role of promoters and enhancers. *J Cell Biochem* 95, 506-517 (2005).

19 Sudhakar, S., Li, Y., Katz, M. S. & Elango, N. Translational regulation is a control point in RUNX2/Cbfa1 gene expression. *Biochem Biophys Res Commun* 289, 616-622 (2001).

20 Banerjee, C. *et al.* Differential regulation of the two principal Runx2/Cbfa1 n-terminal isoforms in response to bone morphogenetic protein-2 during development of the osteoblast phenotype. *Endocrinology* 142, 4026-4039 (2001).

21 Tahirov, T. H. *et al.* Structural analyses of DNA recognition by the AML1/Runx-1 Runt domain and its allosteric control by CBFbeta. *Cell* 104, 755-767 (2001).

22 Yoshida, C. A. *et al.* Core-binding factor beta interacts with Runx2 and is required for skeletal development. *Nat Genet* 32, 633-638 (2002).

23 Kundu, M. *et al.* Cbfbeta interacts with Runx2 and has a critical role in bone development. *Nat Genet* 32, 639-644 (2002).

24 Miller, J. *et al.* The core-binding factor beta subunit is required for bone formation and hematopoietic maturation. *Nat Genet* 32, 645-649 (2002).

25 Guo, Y., Maillard, I., Chakraborti, S., Rothenberg, E. V. & Speck, N. A. Core binding factors are necessary for natural killer cell development

and cooperate with Notch signaling during T-cell specification. *Blood* 112, 480-492 (2008).

26 Tachibana, M. *et al.* Runx1/Cbfbeta2 complexes are required for lymphoid tissue inducer cell differentiation at two developmental stages. *J Immunol* 186, 1450-1457 (2011).

27 Kurebayashi, S. *et al.* Retinoid-related orphan receptor gamma (RORgamma) is essential for lymphoid organogenesis and controls apoptosis during thymopoiesis. *Proc Natl Acad Sci U S A* 97, 10132-10137 (2000).

28 Ivanov, II *et al.* The orphan nuclear receptor RORgammat directs the differentiation program of proinflammatory IL-17+ T helper cells. *Cell* 126, 1121-1133 (2006).

29 Yokota, Y. *et al.* Development of peripheral lymphoid organs and natural killer cells depends on the helix-loop-helix inhibitor Id2. *Nature* 397, 702-706 (1999).

30 Stewart, M. *et al.* Proviral insertions induce the expression of bone-specific isoforms of PEBP2alphaA (CBFA1): evidence for a new myc collaborating oncogene. *Proc Natl Acad Sci U S A* 94, 8646-8651 (1997).

31 Zhang, S. *et al.* Dose-dependent effects of Runx2 on bone development. *J Bone Miner Res* 24, 1889-1904 (2009).

32 Carmeliet, P. *et al.* Abnormal blood vessel development and lethality in embryos lacking a single VEGF allele. *Nature* 380, 435-439 (1996).

33 Meyers, E. N., Lewandoski, M. & Martin, G. R. An Fgf8 mutant allelic series generated by Cre- and Flp-mediated recombination. *Nat Genet* 18, 136-141 (1998).

34 Nagy, A. *et al.* Dissecting the role of N-myc in development using a single targeting vector to generate a series of alleles. *Curr Biol* 8, 661-664 (1998).

35 Lou, Y. *et al.* A Runx2 threshold for the cleidocranial dysplasia phenotype. *Hum Mol Genet* 18, 556-568 (2009).

36 Lazarevic, V. *et al.* T-bet represses T(H)17 differentiation by preventing Runx1-mediated activation of the gene encoding RORgammat. *Nat Immunol* 12, 96-104 (2011).

37 Moro, K. *et al.* Innate production of T(H)2 cytokines by adipose tissue-associated c-Kit(+)Sca-1(+) lymphoid cells. *Nature* 463, 540-544,

(2010).

38 Takeda, S., Bonnamy, J. P., Owen, M. J., Ducy, P. & Karsenty, G. Continuous expression of Cbfa1 in nonhypertrophic chondrocytes uncovers its ability to induce hypertrophic chondrocyte differentiation and partially rescues Cbfa1-deficient mice. *Genes Dev* 15, 467-481 (2001).

39 Komori, T. Regulation of bone development and extracellular matrix protein genes by RUNX2. *Cell Tissue Res* 339, 189-195 (2010).

40 Komori, T. Requisite roles of Runx2 and Cbfb in skeletal development. *J Bone Miner Metab* 21, 193-197 (2003).

Part2: Analysis of bone development of *P2Runx2*$^{neo/neo}$ mice

2.1 Introduction

Runx2 was identified as the causative gene of Cleidocranial Displasia (CCD) in 1997. Patients of CCD exhibit delayed closure of cranial suture, supernumerally teeth and defective development of clavicle[1]. All of the patients show craniofacial bone malformation. Most of them have *RUNX2* gene mutation, which would be the disease triggering nonsense and frameshift mutation[2]. Discovery of Runx2 as the bone controlling transcription factor was accompanied with establishment of two strains of Runx2-null mice, whose homozygous mice displayed complete lack of ossification in whole body skeletons and died soon after birth because of inability of breathing[3,4]. These severe phenotypes of knockout mice suggested that Runx2 plays indispensable roles in both intramembranous and endochondral bone formation.

Most of the researches on the isoforms of Runx2 focused on only P1Runx2 so far because P1 is assumed to be the dominant isoform in bone formation due to its highly limited expression pattern in bone tissue and the results suggesting that P1 isoform is upregulated toward the final

development of osteogenesis *in vitro* and *in vivo*[5,6]. And the location of specific exon(s) of *P1Runx2*, which is far from common exons for both isoforms, makes it easier to generate gene manipulated mice in the P1 specific manners than P2. Actually, this fascinating feature of gene construct drove researchers to establish two P1Runx2 knockout murine models, which showed milder bone defect than two Runx2-null strains; one of them showed only 20% survival rate at 3 weeks of age while the other showed 100% survival[7,8]. Thus it can be said that P1Runx2 has roles in bone formation but not necessarily indispensable.

The way how each Runx2 isoform works attracts much attention, but this problem is difficult to solve because 3-dimensional bone formation is less reproducible *in vitro*, meaning examination of each functional domain of this protein needs an individual mouse model. In spite of this difficulty, many attempts have been performed to explain the function of Runx2 by focusing on its specific functional domains. Prominent one of them is the study with gene manipulated mouse, showing that deletion mutant of subnuclear translocational NMTS signal motif resulted in fetal lethality of homozygote mice[9]. This result clearly shows that this domain works *in vivo* and

necessary for Runx2 function. The attempts indirectly revealing the importance of highly conserved Runt Homology Domain (RHD) by rescuing the fetal lethality of Cbfβ deficient mice are worth noting. Although Cbfβ deficiency causes fatal hematopoietic defect, 3 studies showed Cbfβ deficient mice would suffer from fatal bone malformation when they overcome hematopoietic defect in various methods[10-12]. These reports suggest the importance of RHD of Runx2 because the function of Cbfβ, which does not have DNA binding domain with itself, can only be achieved by making complex with Runx via RHD. This binding changes 3-dimentional conformation of Runx and confers enough DNA binding affinity to Runx[13]. In addition, the fact that mapped mutation of Runx2 gene in CCD patients is mainly located at the RHD also implies that this part of Runx2 contains functionally significant sequence[2].

Each Runx isoforms has unique amino acid sequence at the N-terminal ends but there have not been any positive evidences reported about the function of those terminal structures. Considering that P2 specific sequence is only 5 amino acids long (87 AAs for P1), it is not expectable that unique P2 N-terminal plays any distinctive roles.

Then, why are there evolutionally preserved two isoforms in Runx2? One of the plausible answers of this question can be "dose-dependent function hypothesis". Neomycin resistant cassette insertion into intron between exon7 and 8 of Runx2 compromised the exon splicing, resulting in the generation of hybrid mRNA of *Runx2* and *neo*[r][14]. This alternative splicing resulted in 30% decrement of total *Runx2* gene transcripts which caused slight delay of bone formation in homozygous mice. Because the mice, which are heterozygote for this hypomorphic allele and thus expressed approximately 15 - 20% decreased *Runx2*, did not show any defect in ossification, they discussed that more than 79% expression of wild type *Runx2* is necessary for normal bone formation. In addition to this, another group reported that Runx2 dose determines degree of bone formation. Intercrossing Runx2-null allele possessing mice and P1Runx2-null allele possessing mice constituted gradually Runx2 decreasing series of gene mutated mice, which exhibited increasing severity of bone malformation according to the decreasing gene dosage[6]. This result also suggested that the gene dosage of total Runx2, regardless of its isoforms, affects the extent of bone maturation in vivo. These reports suggested that Runx2 regulates bone

formation in dose dependent way.

The other expectable answer for the question "why Runx2 consists of conserved two isoforms" is that each variant has distinctive role. Expression of P1 isoform is upregulated toward bone maturation *in vitro*[5] and *in vivo*[8]. Although P1Runx2 knockout mice showed largely ossified bone structure and much less sever lethality than Runx2-null mice[7,8], together with the fact that P1 is bone-related isoform of Runx2[5,15], it can be plausible to consider P1 as a dominant isoform for bone formation. If it is true, how they can work in the distinctive ways?

A number of reports described the functional similarities of P1 and P2. Both Runx2 isoforms displayed similar transcriptional activities when they are forced to be expressed in the Cbfβ sufficient cells[16]. When ectopically expressed *in vivo* under the control of Col2a1 promoter, P1 and P2 Runx2 contribute similarly to calcification of cartilage[16,17]. In contrast, a study demonstrated that the dependence on co-factor Cbfβ is higher in P2Runx2 than P1 counterpart[18]. However, the evidence for the functional difference is still few. Given that P1 and P2 Runx2 play indistinguishable roles after translation, it is reasonable expectation that the important check point is

transcriptional regulation. Consistently with this view, there have been studies presenting the results of differential regulation for each isoform, especially in the cranial suture formation[19,20]. Most of previous researchers focused on P1Runx2 to show more expansion of P1 transcription following treatments with Bone Morphogenic Protein-2 (BMP-2)[21] or homeobox protein Dlx-5[19,22]. These data imply signal transduction pathway from Transforming Growth Factor-beta (TGF-β)/BMP - Smad induces P1Runx2 expression. In contrast, P2Runx2, which is largely irresponsive to TGF/BMP signaling, is suppressed by Tumor Necrosis Factor-alpha (TNF-α) treatment[23]. Considering these previous reports, the roles of Runx2 isoforms are not determined by their protein construct but by their spatiotemporal transcriptional regulation.

In this section, I decided to make use of *P2Runx2*$^{neo/neo}$ mice, which expresses decreased amount of both isoforms of Runx2, to examine the dose dependent effect of total Runx2 protein. Although I failed to generate P2Runx2 specific knockout mouse, *P2Runx2*$^{neo/neo}$ mouse has notable feature that its Runx2 expression is more defective in P2 isoforms than in P1 counterpart. This unique feature and hitherto unaccomplished mixing ratio

of isoforms showed functional significance of “not bone-related” Runx2 in skeletogenesis. And this mouse is the model of novel decreasing ratio of total Runx2, which reinforces the “dose-dependent hypothesis” of Runx2 function. I confirmed that the lethality of *P2Runx2*$^{neo/neo}$ mice was caused by delayed bone ossification because of the defective osteoblast differentiation. This study provides new pieces for a puzzle of Runx2 function on bone formation.

2.2 Material and Methods

2.2.1 *Preparation of whole body skeletal specimen*

The pregnant maternal mouse was sacrificed and fetal mice were obtained at 18.5 days post-coitum. Fetuses were preserved on the ice cold medium (e.g. RPMI containing NCS 2% - 10%) until dissection. On the beginning of dissection, the fetus was euthanized by quick removal of the heart. In the skeletal analysis, it was impossible to obtain tail chips because whole skeleton, including tail bone, should be kept intact, so some organs (liver or intestine) were used for genotyping instead. All their organs, except for brain, and epidermises were carefully removed. Especially, the extraordinary care was needed for the removal of skins of tips of fingers and tails because the tissue was so fragile to the tension but bone tissue could not be stained if the skins remained. Skins should be cut longitudinally by two ways, and then peeled off softly. After removal of organs and skins, specimens were dehydrated and stocked in the 100% EtOH (10 - 50 ml for each fetus). Staining solution was prepared. Alucian Blue powder was dissolved in 76% EtOH - 20% acetic acid solution; this solution was made from 10 ml glacial acetic acid (Sigma) and 40 ml 95% EtOH (Nacalai) and 7.5 mg of Alucian

Blue 8GX (Sigma). This solution should be rotated at room temperature for at least 1 hour before use. Alucian Blue solution from Nacalai tesque was also tested but it did not stain cartilages efficiently enough. Alizarin Red solution was made by dissolving 1.25 - 3.75 mg Alizarin Red S (Sigma) in 50 ml of 1% KOH solution. Dehydrated fetuses were picked up from EtOH and moved to 6-well plates. Alucian Blue solution was added onto specimens to such an amount that the specimens sank in the solution completely. Specimens were incubated for overnight at room temperature with gentle shaking. After incubation, specimens were quickly washed by 95% EtOH twice, and then 2% KOH solution was added into each well for overnight incubation at room temperature. Because this KOH solution would strongly dissolve the remaining organs and skin of fetuses, this incubation should not exceed 24 hours; it should be even less 20 hours long, otherwise the skeleton would be collapsed. After removing the 2% KOH, Alizarin Red solution was added and incubated for overnight. After this incubation with Alizarin Red, the solution would be back to 2% KOH to bleach and dissolve colored skins and connective tissues. This incubation was ad libitum so as to clean up the specimen enough without breaking the skeletal formation. After cleaning of

specimens, buffer was replaced with 20% glycerol, 1% KOH solution followed by incubation at room temperature for few days. Then, buffer was changed to 20% glycerol, 20% EtOH solution. After overnight incubation, buffer was replaced again with solution of glycerol : EtOH = 1 : 1. Finally, buffer would be 100% glycerol for further preservation. This buffer change steps should not skipped (*e.g.* 2% KOH replacement directly with 20% glycerol, 20% EtOH solution) because newly added chemical contents, such as EtOH, would make so severe convection that could break skeletal architecture. The stained specimens were observed by the stereo microscope. In this microscopic examination, the light should be placed under the specimen (LED light board is preferable) otherwise light placed overhead the specimen would make the shadow, which would make it difficult to distinguish the color contrast of blue and red, beneath the samples. After the observation of whole body skeleton, the specimens were disassembled into each part and further examined.

2.2.2 *Micro CT analysis*

Micro CT analysis was done with great help of Prof. Takayanagi and Dr.

Nakashima in Tokyo Dental and Medical University. Fetuses prepared like in skeletal staining experiments were preserved in 70% EtOH and whole bodies and femurs of them were subjected to micro CT analyses.

2.2.3 *Preparation of calvarial cells from calvarium* .

Pregnant mice were sacrificed to obtain fetus. While the fetuses were preserved on the ice cold medium (e.g. RPMI containing NCS 2% - 10%), digestion α-MEM medium containing 10% FCS, antibiotics, 0.1% collagenase (Wako) and 0.2% dispase (Roche) was prepared for the number of fetuses because it was impossible to know how many fetuses could be obtained before dissection of maternal mouse. Enzymatic digestion was performed in 15 ml vial with small magnetic stirrer. If cell culture was needed, the equipment should be briefly sterilized by exposure to the UV light for several hours before use. At the same time, scissors, tweezers and a number of FACS tubes, which would be for syringe stands, should be sterilized. Here, scissors and tweezers were necessary to be specially designed for elaborate work and small enough to handle tiny fetal calvarial tissues. Prepared digestion medium should be warmed in water bath at 37 degree Celsius. Fetuses were

taken up from womb, in clean benches if it was needed. When genotyping of fetuses is needed, it could be done by using tail chip of fetuses but the experimenter should be careful not to contaminate tissue or blood of maternal origin and from other fetuses. After euthanizing a fetus by amputating its head from the body, the skull was cut off from the head. In this procedure, skin was separated from the skull at first by cutting with scissors in a way forming a circle on the fetus head. And then skull was cut in the same way, picked with tweezers at occipital end and then removed from the head without containing brain tissues. Calvarium was transferred into 15 ml vial soon. At this time, there should be 2 - 3 ml digestion medium in the vial in advance to protect calvarial issue from drying up. After dissection of each fetus, the scissors and tweezers should be cleaned by wiping off remaining tissue and blood with Kimwipe wetted by 70% EtOH. After finishing processing all the fetuses, digestion medium was added up to 3 - 5 ml as the final volume. 3 ml is recommended because one step of centrifugation in later procedure can be skipped by doing so. Enzymatic digestion was conducted in 37 degree Celsius for 10 min for 5 times. Among them, first digestion was discarded as directed in the previous report[24], and

later 4 digestions were pooled for the following procedure. When collecting digestion, large fragments should not be contained into pool. Syringes should be sterilized and stood on sterilized FACS tubes during continuous medium change of vials. After centrifugation of pooled medium at 1500 rpm, 4 degree Celsius for 5 min, supernatant was aspirated off and cells were washed for once with medium without digestion enzymes. After washing, cells were suspended in 2 ml of α-MEM supplemented 10% FCS and antibiotics (highly recommended) and seeded on 6-well plates without counting the cell number. Following three days, cells were expanded on the plate. This expansion period must not exceed three days because pluripotency of calvarial cells would be rapidly lost after three days. And genotyping of fetuses or preparation of culture medium should be done within this period.

2.2.4 *Osteoblast developmental procedure*

Cell were collected from expansion culture plate(s), and counted. To harvest, first culture medium was gently aspirated off and cells were washed by cold PBS. Since these primary calvarial cells attached firmly to culture plate, it was not necessary to care about their detachment. Then, 0.25% Trypsin

(Nacalai), supplied with 0.5 M EDTA 80 μl per 100 ml, was added on the cells and incubated at 37 degree Celsius for 5 min. After the incubation, Trypsin was inactivated by the addition of culture medium. Cells were isolated well into the single cell suspension by pipetting, and were centrifuged in the 10 volume of culture medium at 4 degree Celsius for 5 min. During this centrifugation, cell number was counted by using Trypane Blue solution (Wako). 4×10^5 cells were suspended with osteoblast differentiation medium (α-MEM supplemented with 50 μM ascorbic acid (Wako), 10 nM dexamethasone (Wako) and 10 mM β-glycerophosphate (Tokyo Chemical Industry)) and then plated on 24-well culture plate. The courting quality of culture plates should be evaluated in advance because bottom treatment of culture plate greatly affects the differentiation efficiency of MSCs. Cells were cultured in this setting for 2 weeks. Culture medium was changed every 3 or 4 days until the end of culture period. This medium change should be done with great care so as not to detach cells from the plate bottom. Over grown cells would attach each other to make a sheet of cells, which is so easily detached from plate like being peeled off from it.

2.2.5 *Bone nodule formation assay*

After osteoblastic culture period, cells were subjected to bone nodule formation assay. After aspirating off the culture medium, cells were washed by cold PBS and then fixed by 4% paraformaldehyde - PBS solution at room temperature for 10 min. Because staining without fixation was conducted and exhibited the comparable result to fixed one, this fixation step might be able to be omitted. This notion is further supported by the fact that Alizarin Red staining could be successfully done after lysis of cell. Actually, Alizarin Red solution contains KOH which will lyse cells, thus staining procedure can be conducted regardless of the existence of the cells. After fixation, cells were briefly washed by PBS and Alizarin Red solution was added onto them. Cells were incubated for overnight with gentle shaking. After incubation, Alizarin Red solution was removed and plates were washed by clean water. Then, the stained culture plates were dried up for the examination. Plates were examined under microscope with the light from the bottom of plate just same as the skeletal examination. The number of bone nodules, identified as red purple dots, was counted manually. The discrimination whether a dot is bone nodule or not was conducted by the criteria of size. Dots were compared with

the standard dot in image processing software in PC.

2.2.6 *Alkaline phosphatase assay*

Measurement of alkaline phosphatase activity of differentiated calvarial cells was performed by kit (Wako). The experimental procedure largely followed manufacturer's instruction. Here, I note the steps different from the official protocol. After washing by ice cold PBS, 200 μl of 0.05% Triton X were added on the cells which were placed on the ice. Culture plates with cells and lysis buffer were frozen at -80 degree Celsius directly for preservation. Before lysate samples were collected from plates, samples underwent one more set of freeze and thaw, which is believed to enhance alkaline phosphatase activity. After total two freeze-thaw cycles, the lysates were transferred into 1.5 ml tubes with gentle pipetting for several times. Lysate was centrifuged at 14,000 rpm, 4 degree Celsius for 15 min and supernatant was transferred into a new tube. Enzymatic reaction of alkaline phosphatase was conducted in the immunoplate (NUNC) so as to avoid any troubles in reading the absorbance of the light of 405 nm wave length by micro plate reader. Both ×10 and ×100 dilution series were prepared in case the

absorbance of sample gets out from the standard curve, and this made the experiments successful for wild type sample (absorbs higher) and *P2Runx2*$^{neo/neo}$ sample (absorbs lower). All samples were measured as singlet because no less than two culture wells were prepared from calvarial cells of each mouse.

2.2.7 *Quantitative PCR*

Primer sets used in experiments of this section are as shown below.

Gene		Sequence
Alpl	Fw	5'-cggatcctgaccaaaaacc-3'
	Rv	5'-tcatgatgtccgtggtcaat-3'
Bglap	Fw	5'-agactccggcgctacctt-3'
	Rv	5'-ctcgtcacaagcagggttaag-3'
Col1a1	Fw	5'-catgttcagctttgtggacct-3'
	Rv	5'-gcagctgacttcagggatgt-3'
Tnfsf11	Fw	5'-tgaagacacactacctgactcctg-3'
	Rv	5'-ccacaatgtgttgcagttcc-3'
Sp7	Fw	5'-cgtcctctctgcttgaggaag-3'

	Rv	5’-gccgccaaatttgctgcagg-3’
Gapdh	Fw	5’-tgtccgtcgtggatctgac-3’
	Rv	5’-cctgcttcaccaccttcttg-3’

PCR cycle for qPCR of these genes were

<----------45 cycles----------> Melting curve

95℃ 5min 95℃ 10sec 60℃ 10sec 72℃ 10sec

The preciseness of amplification was examined by melting curve analysis and sequence analysis of amplicon. The amount of each gene product was normalized by the amount of transcripts of internal control gene *Gapdh*.

2.3 Results

2.3.1 *Isoform specific expression of Runx2 in calvarial cells were inconsistent with previous results*

P1Runx2 is hypothesized to be the dominant isoform of Runx2 in bone formation[5,6]. This hypothesis is based on *in vitro* experiment, showing increased amount of *P1Runx2* expression at later stages of osteoblast development[5], and *in vivo* experiment of similar results[6] and the fact that P1 isoform is bone specifically expressed in the bone[5,15]. But these evidences were not conclusive. *In vitro* upregulation of P1 should exclude the possibility that Runx2 was induced by the effect of arrested cell cycle because Runx2 expression was reported to be promoted when cell culture reaches confluent[25]. And, in the report on *in vivo Runx2* expression, the authors made use of whole body lysate of fetuses[6]. This is problematic because P2 isoform is expressed in whole body and their result, showing growing expression level of P1 isoform toward birth, could just reflect the changing ratio of osseous and non-osseous tissues.

Therefore I decided to challenge this issue in the more precise way, where I purified calvarial cells from fetuses of each embryonic day for the

quantification of *Runx2* gene expression isoform specifically. In this experiment, I tried to pick calvarium from mice of embryonic days, E11.5 and E13.5 fetuses, however, had not developed the definitive calvarial tissues. Instead, I collected the crude upper head including calvaria, brain, skin and any other cells for references. The results clearly showed, in contrast to the previous report, that both isoforms of *Runx2* are expressed constantly in calvarium throughout embryonic days and total *Runx2* level is maintained (Figure10). This result implies the necessity to re-examine the "common sense" of gene regulation in bone development.

2.3.2 *Further examination of Runx2 expression in P2Runx2$^{neo/neo}$ mouse*

Although the gene interrupting *neo^r* insertion was in the intron of common region for P1 and P2 *Runx2*, *P2Runx2$^{neo/neo}$* mouse does not show equal decrement of gene transcript of *Runx2* isoforms. Therefore, it is worth examining how each variant is expressed in calvaria of *P2Runx2$^{neo/neo}$* mouse and its littermates. The ratios of expression are calculated from the raw data of Figure5 and 8, and shown in Table1. Despite more than 80% of *P2Runx2* was lost in homozygote, 40% *P1Runx2* was still kept in wild type. I do not

know the absolute amount of each *Runx2* isoform because qPCR was done as relative quantification and the levels of signal depend much on the design of primers. Therefore, I calculated the amount of each isoform by using these decrements of expression of isoforms and total *Runx2*. Given that total *Runx2* is provided from summation of P1 and P2 isoforms, the decrement of total *Runx2* is also provided from decrements of P1 and P2 isoforms. But simple average of expression level of P1 and P2 (0.29) is not equal to that of total Runx2 (0.33), since the original amounts of P1 and P2 isoform are different, where amount of P1 is expected to be more than P2. From this notion, making unknown value x as percentage of how much P1 expression exceeds that of P2, the equation (1) holds. Solving this, the solution is 0.88 (88%). This result provides more correct understanding what occurs in *P2Runx2*$^{neo/neo}$ mouse. Using this result, I further calculated the contribution of one copy of *Runx2* isoform for total *Runx2*. Because total *Runx2* is sum of P1 and P2 isoforms (*), given unknown value y as the contribution of one allele of P2 isoform, the equation (2) holds. Solving this equation, the contribution of P2 is given as 17.2% and P1 is 32.8%. These results should be applicable for other studies and will account for their observations which are

not yet explained well.

2.3.3 *Osteogenic gene expression*

Lethality of *P2Runx2*$^{neo/neo}$ mice was presumably due to bone malformation similar to Runx2 null mice. To address this possibility, first I examined the amount of gene transcripts which are known as osteoblast maturation markers. For quantitative PCR following reverse transcription of total RNA was performed with primers designed by Roche web site or by myself. Primers were set so that they flank intron, the length of amplicon should be no longer than 120 bp and the melting temperature should be around 60 degree Celsius. Alkaline phosphatase (*Alpl*), Osteocalcin (*Bglap*), Type I Collagen (*Col1a1*), Osterix (*Sp7*) and RANKL (*Tnfsf11*) were examined. Among them were *Alpl* and *Tnfsf11* which showed significant decrease in *P2Runx2*$^{neo/neo}$ mice compared to wild type littermates (Figure11). *Col1a1* and *Sp7* showed substantial but not significant decrement in homozygote. *Bglap* was the only osteogenic gene which did not display the decreasing tendency in *P2Runx2*$^{neo/neo}$. These results strongly suggest that *P2Runx2*$^{neo/neo}$ mice have the phenotype of defective bone formation resulted

from insufficient osteoblast differentiation.

Beside that notion, it was interesting to see the reason why *Bglap* (Osteocalcin), whose promoter has strong Runx binding element (OSE2)[26], did not exhibit any reduction of gene expression. To address this issue, I performed qPCR of these genes with templates prepared from wild type embryonic mice (Figure12). From the results, I found rapid induction of *Bglap* between E17.5 and E18.5 while Runx2 expression is almost the same (Figure10). Such an exponential induction of *Bglap* means that just a slight difference of examination time point can result in the great difference of the detected amount of gene transcript. Based on this notion, I called CLEA Japan Inc., from which I purchased pregnant mice used in this experiment, to clarify their time points of plug check. They informed me that they put mating couples together at 2 p.m. and check intercourse at 8 a.m. I usually control the same procedure from 8 p.m. to 10 a.m., and then there exists 6 hours gap of age between fetuses of CLEA Japan and mine. Because the mice which I prepared were 6 hours younger than purchased ones, the induction of *Bglap* had not been fully driven in my mice and thus the result did not show significant difference of *Bglap* gene expression between wild type and

P2Runx2$^{neo/neo}$ mice.

2.3.4 *Bone ossification is defective in P2Runx2*$^{neo/neo}$ *mice*

To confirm whether decreased osteogenic gene expression is the consequence from defective osteoblast development *in vivo*, I prepared whole body skeletal specimens of E18.5 fetus and stained them with Alizarin Red which marks ossified bone and Alucian Blue for cartilage (Figure13). *P2Runx2*$^{neo/neo}$ mice exhibited severely delayed skeletal development obvious at intramembranously formed bone such as cranial suture, clavicle and occipital bone. The fontanelles of *P2Runx2*$^{neo/neo}$ mice remained wider than wild type and they completely lacked clavicle and occipital bone formation. Also at long bones, *P2Runx2*$^{neo/neo}$ mice showed delayed ossification. Their hyoid bones did not have center calcified zone and the number of ossification centers of phalangel bone was fewer in *P2Runx2*$^{neo/neo}$ than in wild type littermates.

For quantification of delayed bone formation of *P2Runx2*$^{neo/neo}$ mice, femurs of mice from each genotype were subjected to micro CT analysis (Figure14). Figures of CT scanning showed severe delay of ossification

especially in skull of *P2Runx2*$^{neo/neo}$ mouse (Figure14 A). In bone volume per tissue volume, trabecular thickness and trabecular number *P2Runx2*$^{neo/neo}$ mice showed decreased values and their trabecular separation and trabecular spacing were increased significantly compared to wild type and heterozygote. These changed parameters all indicated defective bone formation of *P2Runx2*$^{neo/neo}$ mice. Unexpectedly, heterozygotes did not exhibit any defective changes in this examination while their gene expression profiles and morphological appearances were intermediate between wild type and homozygote.

2.3.5 *Osteoblast development is defective in P2Runx2*$^{neo/neo}$ *mice*

In vivo phenotypes of *P2Runx2*$^{neo/neo}$ mice showed defective bone formation. In order to confirm whether this is the consequence of inability of mesenchymal stem cells (MSCs) to develop into osteoblast, I performed *in vitro* osteoblast differentiation assays. Cells were prepared from enzymatically digested fetal calvarium and cultured in the osteoblast differentiation medium for 2 weeks. After the culture period, wild type cells formed bone nodules which can be stained by Alizarin Red and showed

alkaline phosphatase activity which is the marker of mature osteoblasts (Figure15). In contrast, cells from *P2Runx2*$^{neo/neo}$ mice formed less number of bone nodules and significantly weaker activity of alkaline phosphatase than control cells. These results strongly suggest that *P2Runx2*$^{neo/neo}$ cells are defective in osteoblast differentiation and, as a result, lead fatal malformation of skeleton. Of note, heterozygous cells showed intermediate activities again in these assays, suggesting that in the 2-dimentional artificial differentiation system the available Runx2 amount linearly correlates with cell differentiation efficiency.

2.4 Discussion

With two different isoforms which are supposed to be functionally identical, Runx2 play essential roles in bone development. In spite of intensive researches performed for 15 years since the first identification of Runx2 as a master regulator of osteoblast development, how each isoform works remains largely unknown until today. One of the biggest reasons for this is the lack of mouse model which specifically focused on P2Runx2. Because specific coding sequence is only 16 bp and whole P2 specific exon, which includes 5' UTR and is directly connected to common exon for P1 and P2, is 1029 bp long, it is quite difficult to manipulate P2Runx2 specifically. Previous studies with mouse models of manipulated P1Runx2 showed that this isoform is important for completion of skeletal development but not necessary for mouse survival[7,8]. These observations fueled the discussion about the roles of Runx2 isoforms. There is no evidence for the functional difference between these two isoforms, and a report showed the similar effect of ectopic expression of both Runx2[16]. Thus, current major hypothesis is "dose-dependent hypothesis", in which both Runx2 work in the same way and the total amount of Runx2 determines the cell fate[6].

The biggest difference between two Runx2 isoforms is not their N-terminal amino acid construct but their regulation. Their expression pattern is different in space[19,20] and time[6]. First, I challenged the latter by examining the *Runx2* expression level in bone development more precise way than previous report[6], and found the expression of both *Runx2* isoforms are constant throughout the embryonic development (Figure10). Based on this data, the notion that P1Runx2 is a dominant isoform in bone formation is not simply applicable for *in vivo* development. Probably, previous observation was just the reflection of developing endochondral ossified bones, where P1Runx2 is thought to be more active than P2[27]. In addition, considering the article which showed that Runx2 is upregulated to arrest cell growth when the culture reaches confluent[25], the *in vitro* observation of increasing P1Runx2 expression toward the final osteoblast differentiation can be artifact from the effect of cell overgrowth.

Determination of expression levels of *Runx2* isoforms and their contribution to total *Runx2* level is important to place this study in series of Runx2 researches. To achieve this end, I re-examined the data of gene quantification (Table1). I calculated the ratio of *Runx2* transcripts of each

genotyped mouse to that of wild type, and found that nearly 85% of *P2Runx2* was lost in *P2Runx2*$^{neo/neo}$ mouse while only 58% of *P1Runx2* was lost. From this result, although *P2Runx2*$^{neo/neo}$ mice show significant decrement in both P1 and P2 *Runx2*, almost the half of *P1Runx2* is revealed to be still expressed. The reason of this biased decrement is not clear. There is a mini review suggesting that *neo*^{r} may interfere the expression of neighboring genes, presumably owing to the interaction with adjacent promoters or enhancers[28]. Taking this notion into consideration, it is not strange that P2 promoter, which is closer to *neo*^{r} than P1 promoter, is affected more by *neo*^{r}. This uneven decrement of isoforms enabled me to calculate the absolute ratio of P1/P2 transcripts. Simple equation gave the solution that P1 transcript is expressed almost 90% as much as that of P2 (Table1). Although I once denied the previous concept that P1 is dominant isoform for the skeletal development, that hypothesis can be partly true in terms of abundance of gene transcripts.

The determination of absolute amount of RNA is essential for comparison of phenotype of *P2Runx2*$^{neo/neo}$ mouse with previous reported *Runx2* manipulated mouse models. Making use of result of calculation, I

further computed the contribution of single allele of *Runx2* isoform. Solving the equation, P1 was given as 32.8% and P2 as 17.2% (Table1). The accuracy of calculation is certified by applying obtained parameters to results from heterozygote. 18% decrement of P1 isoform and 53% decrement of P2 are summed up to 29.96% of total *Runx2*, which equals to experimentally determined amount of total Runx2 (30%). This confirmation also guarantees the appropriate experimental procedures. These results will help us to understand previous report showing that $P1^{+/-}P2^{+/-}$ and $P1^{-/-}P2^{+/+}$ mice gave different outcomes[6]. The authors discussed why these two mice models, though both lack the half of total Runx2 gene copies, showed different phenotypes ($P1^{-/-}P2^{+/+}$ results in 80% perinatal death whereas $P1^{+/-}P2^{+/-}$ shows no sign of death), and they attributed this phenomenon to the unknown functional difference between two isoforms. But, applying my observation to their results, $P1^{-/-}P2^{+/+}$ mouse should have 67% of wild type *Runx2* amount. Importantly, despite the half of *Runx2* alleles were inactivated in this mouse, the authors showed in their previous report that $P1Runx2^{-/-}$ mouse expresses twice as much *P2Runx2* expression as wild type mouse do and this should result in slightly higher expression of total *Runx2*

amount than that of expected[7]. This is assumed to be because of compensatory mechanism of *Runx2*, as implied in another report as suppressive autoregulation of *Runx2*[29]. The authors of *P1Runx2*$^{-/-}$ report almost ignored the effect of *P2Runx2* induction, because, if P1 and P2 are expressed in the same amount, doubled expression of P2 would totally mask the lack of P1 isoform. The fact that their result could make sense by applying my idea also supports the reliability of my study indirectly. The compensatory mechanism similarly should work in P1$^{+/-}$P2$^{+/-}$ mouse, but quantified gene amount was not shown in related reports. Judging from the phenotype without lethality, P1$^{+/-}$P2$^{+/-}$ mouse produces total *Runx2* more than 67% of wild type[3,6]. There are many reports which did not show the amount of *Runx2* transcript of their original mice. I suppose that they decided not to release their gene examination data because it can be interpreted as the failure of gene targeting (*e.g.* *Runx2*$^{+/-}$ mouse expresses *Runx2* more than 50% of wild type). But, in order to promote the understanding the Runx2 function on dose-dependent hypothesis, precise examination of gene amount of each isoform is necessary. I would like to put *P2Runx2*$^{neo/neo}$ into the series of *Runx2* mutated mice as 67% *Runx2* deficient

mice.

The mouse model generated in this study is the novel and unique one in the history of Runx2 investigation, since *P2Runx2*$^{neo/neo}$ mouse lacks *P2Runx2* prior to P1 counterpart and shows severe defect in intramembranous ossification, implying the central involvement of P2Runx2 in intramembranous ossification. This notion is consistent with the previous report which suggested the distribution of roles for Runx2 isoforms according to the part of body[27]. Considering the differential expression pattern of each isoform in cranial suture formation, it is easily expectable that each isoform has distinctive function. The important thing is keeping it in mind that the functional specificities are not evolved from protein construct but expressional regulation as discussed below. Although *P2Runx2*$^{mut/mut}$ mouse (described in Part1) expresses P2Runx2 without specific N-terminal amino acid sequence, this mouse shows no defect in survival, suggesting this unique sequence does not have any important roles for survival and presumably for bone formation. Considering these observations on *P2Runx2*$^{neo/neo}$ mouse, further investigation of this mouse model will provide many valuable insights about the function of Runx2, especially about

P2Runx2. The novel finding about P2 isoform is of great value. Because a portion of CCD patients do not have any mutations in their Runx2 coding region, the suspicion that they have mutations in promoter sequence for Runx2 would arise theoretically[30]. There is already a report about examination of such a possibility, but the authors focused only on P1 promoter and could not find effective regulatory elements[30]. Considering the previous report, together with this study, it will be fruitful to examine P2 promoter of CCD patients. For this purpose, I am preparing the P2 promoter reporter vectors to test their transactivation abilities.

Several osteogenic gene expressions were revealed to be decreased in *P2Runx2*$^{neo/neo}$ calvarium than that of wild type (Figure11). But these changes were more moderate than those expected from the severe lethal phenotype of this mouse. This is partly because of incomplete lack of total Runx2. And another speculation induced from this result is that partial decrement of gene expression can lead severe consequence in bone formation. Because skeletal development needs quite a long time spanning before and after birth, meaning stable expression of regulatory elements during this period is necessary for the completion of skeletal development. This notion is

consistent with the fact that clavicle, whose formation begins at the earliest time point and continues for longest duration[31], is one of the most susceptible bones to altered osteogenic gene expression[14]. These results and interpretation will be helpful for understanding of dose dependent bone formation and different phenotypes of bone malformation according to the part of body.

The osteocalcin gene expression did not show large difference between wild type and *P2Runx2*$^{neo/neo}$ mice (Figure11). This result was of great interest for me because osteocalcin is the standard gene known by its promoter region containing highly responsive oligo nucleotide sequence, named OSE2, for Runx2, and used for numerous reporter assay studies for Runx2 binding[26]. Therefore, I examined the expression profiles of osteogenic genes during embryonic development and found osteocalcin as the most rapidly induced gene in calvarium at the end of fetal period (Figure12). Since the amount of *Runx2* transcript was not changed throughout this period (Figure10), there must be other factor(s) which induce osteoclacin expression. One of such factors might be vitamin D_3, which enhances osteocalcin expression after its expression starts[32]. Rapid induction means that slight

gap of examination time point can be result in the great difference of detectable gene abundance. This fact drove me to ask CLEA Japan Inc., which provided the pregnant mice tested at wild type fetal gene expression profiling experiment, when they do mouse mating and plug checking. Their answer was one just as I had expected that the mice mating time in their facilities is from 2 p.m. to 8 a.m., whereas I did it from 8 p.m. to 10 a.m., that is 6 hours later than they do. This gap of time point is not negligible when I examine the expression of rapidly induced genes such as osteocalcin. From these results and information, I concluded that unaffected osteocalcin expression is due to the examination time point which was slightly earlier than that of the peak of osteocalcin induction.

To verify the defect of ossification in *P2Runx2*$^{neo/neo}$ mice, the whole skeletal bone specimens were prepared from embryos at 18.5 days from gestation. The results showed severe delay of ossification, observed typically in intramembranous ossified bones such as calvarium and clavicles (Figures 12 and 13 A). Open fontanelle, the consequence of delayed cranial suture closure, was obvious in homozygote and occipital bone was completely lost from *P2Runx2*$^{neo/neo}$ mice. No clavicle was observed in *P2Runx2*$^{neo/neo}$ mice.

These phenotypes are in consistent with previous reports and the notion that intramembranous ossification process is more sensitive to decreased Runx2 amount than endochondral counterpart, illustrated by the notable defect in intramembranous ossification of CCD patients. Delayed bone formation is also obvious in endochondrally ossified bones, exemplified by the lack of calcification in hyoid bone and the reduced number of ossification center in phalanxes. The delayed bone formation was further confirmed quantitatively by micro CT analysis. All of the parameters significantly changed between wild type and homozygous mice, showing ineffectiveness of bone formation in *P2Runx2*$^{neo/neo}$ mice (Figure13 B). Of note, heterozygous mice, which exhibited intermediate phenotype between wild type and homozygote in gene expression and morphological analyses, showed indistinguishable value in each parameter from that of wild type. μCT measurement was performed by using femurs which are endochondrally ossified. As I mentioned above, intramembranous ossified bones are more sensitive to the decrement of Runx2 transcript, as seen in human CCD patients, and this might be also applicable to gene manipulated mice. It is also possible that P2Runx2 is mainly responsible for intramembranous ossification while P1 is for

endochondral ossification[27]. In fact, mice totally lacking Runx2 expression showed ossification in their tibias, radius and ulnas[4,6]. Therefore, it is reasonable to suppose that there are some redundant or bypassing mechanisms over Runx2 in long bones, or that other transcription factors, than Runx2, are more important in the ossification of some long bones. The result obtained in this study would be one of the evidences for the existence of such mechanisms.

To further confirm that the delayed bone formation is the consequence of defective osteoblast development, in vitro differentiation assays were performed. After culture period in the osteoblast differentiation medium, wild type calvarial cells differentiated into osteoblast to form bone nodules and to show strong alkaline phosphatase activity, while cells derived from *P2Runx2*$^{neo/neo}$ calvarium exhibited significantly lower activities in both assays (Figure14). These results gave certification of defective osteoblast genesis in homozygote mice. The attracting observation is, again, the phenotype of heterozygous cells, which showed intermediate phenotype in these assays. There can be two possibilities for this observation; 1) the result here reflects the origin of cells, intramembranously ossified calvarium which

is sensitive for Runx2 amount in dose-dependent way. 2) 2-dementional *in vitro* experiment does not mimic 3-dementional *in vivo* osteoblast genesis well. This is an important notion because, until today, many of examinations about the function of Runx2 have been performed *in vitro* experimental settings, using calvarial cells or cell lines, which might not reflect *in vivo* 3-dimentional bone formation well. To make definitive conclusion for this issue, experiments using MSCs derived from endochondrally ossified bones are needed.

In conclusion, I established novel mouse model *P2Runx2*$^{neo/neo}$, which lacks 67% of total *Runx2* and shows remarkable phenotype including inescapable lethality. These results provide new insight into both Runx2 dose-dependent hypothesis and isoform specific working hypothesis. And, by utilizing the uneven decrement of each isoform, I calculated the absolute ratio of P1/P2 isoform, which further helps the comprehension of phenotypes of previously established mice. In addition, *P2Runx2*$^{neo/neo}$ mouse is more defective in *P2Runx2* rather than P1 counterpart. This is the notable feature which has not been accomplished. Although this study greatly contributes to the series of *Runx2* research, there still remains huge amount of questions

about *Runx2* function. Extensive efforts, which are focused especially on the dose dependency and long neglected P2 isoform, should be continued until total understanding of bone formation. Such firm knowledge will be of fabulous value in clinical application.

2.5 References

1 Mundlos, S. *et al.* Mutations involving the transcription factor CBFA1 cause cleidocranial dysplasia. *Cell* 89, 773-779 (1997).

2 Yoshida, T. *et al.* Functional analysis of RUNX2 mutations in Japanese patients with cleidocranial dysplasia demonstrates novel genotype-phenotype correlations. *Am J Hum Genet* 71, 724-738 (2002).

3 Otto, F. *et al.* Cbfa1, a candidate gene for cleidocranial dysplasia syndrome, is essential for osteoblast differentiation and bone development. *Cell* 89, 765-771 (1997).

4 Komori, T. *et al.* Targeted disruption of Cbfa1 results in a complete lack of bone formation owing to maturational arrest of osteoblasts. *Cell* 89, 755-764 (1997).

5 Banerjee, C. *et al.* Differential regulation of the two principal Runx2/Cbfa1 n-terminal isoforms in response to bone morphogenetic protein-2 during development of the osteoblast phenotype. *Endocrinology* 142, 4026-4039 (2001).

6 Zhang, S. *et al.* Dose-dependent effects of Runx2 on bone development. *J Bone Miner Res* 24, 1889-1904 (2009).

7 Xiao, Z. S., Hjelmeland, A. B. & Quarles, L. D. Selective deficiency of the "bone-related" Runx2-II unexpectedly preserves osteoblast-mediated skeletogenesis. *J Biol Chem* 279, 20307-20313 (2004).

8 Liu, J. C. *et al.* Runx2 protein expression utilizes the Runx2 P1 promoter to establish osteoprogenitor cell number for normal bone formation. *J Biol Chem* 286, 30057-30070 (2011).

9 Choi, J. Y. *et al.* Subnuclear targeting of Runx/Cbfa/AML factors is essential for tissue-specific differentiation during embryonic development. *Proc Natl Acad Sci U S A* 98, 8650-8655 (2001).

10 Yoshida, C. A. *et al.* Core-binding factor beta interacts with Runx2 and is required for skeletal development. *Nat Genet* 32, 633-638 (2002).

11 Kundu, M. *et al.* Cbfbeta interacts with Runx2 and has a critical role in bone development. *Nat Genet* 32, 639-644 (2002).

12 Miller, J. *et al.* The core-binding factor beta subunit is required for bone formation and hematopoietic maturation. *Nat Genet* 32, 645-649

(2002).

13 Tahirov, T. H. *et al.* Structural analyses of DNA recognition by the AML1/Runx-1 Runt domain and its allosteric control by CBFbeta. *Cell* 104, 755-767 (2001).

14 Lou, Y. *et al.* A Runx2 threshold for the cleidocranial dysplasia phenotype. *Hum Mol Genet* 18, 556-568 (2009).

15 Sudhakar, S., Li, Y., Katz, M. S. & Elango, N. Translational regulation is a control point in RUNX2/Cbfa1 gene expression. *Biochem Biophys Res Commun* 289, 616-622 (2001).

16 Ueta, C. *et al.* Skeletal malformations caused by overexpression of Cbfa1 or its dominant negative form in chondrocytes. *J Cell Biol* 153, 87-100 (2001).

17 Takeda, S., Bonnamy, J. P., Owen, M. J., Ducy, P. & Karsenty, G. Continuous expression of Cbfa1 in nonhypertrophic chondrocytes uncovers its ability to induce hypertrophic chondrocyte differentiation and partially rescues Cbfa1-deficient mice. *Genes Dev* 15, 467-481 (2001).

18 Kanatani, N. *et al.* Cbf beta regulates Runx2 function isoform-dependently in postnatal bone development. *Dev Biol* 296, 48-61 (2006).

19 Lee, M. H. *et al.* Dlx5 specifically regulates Runx2 type II expression by binding to homeodomain-response elements in the Runx2 distal promoter. *J Biol Chem* 280, 35579-35587 (2005).

20 Park, M. H. *et al.* Differential expression patterns of Runx2 isoforms in cranial suture morphogenesis. *J Bone Miner Res* 16, 885-892 (2001).

21 Lee, K. S. *et al.* Runx2 is a common target of transforming growth factor beta1 and bone morphogenetic protein 2, and cooperation between Runx2 and Smad5 induces osteoblast-specific gene expression in the pluripotent mesenchymal precursor cell line C2C12. *Mol Cell Biol* 20, 8783-8792 (2000).

22 Chen, G., Deng, C. & Li, Y. P. TGF-beta and BMP signaling in osteoblast differentiation and bone formation. *Int J Biol Sci* 8, 272-288 (2012).

23 Gilbert, L. *et al.* Expression of the osteoblast differentiation factor RUNX2 (Cbfa1/AML3/Pebp2alpha A) is inhibited by tumor necrosis

factor-alpha. *J Biol Chem* 277, 2695-2701 (2002).

24 Ogata, N. *et al.* Insulin receptor substrate-1 in osteoblast is indispensable for maintaining bone turnover. *J Clin Invest* 105 (2000).

25 Pratap, J. *et al.* Cell growth regulatory role of Runx2 during proliferative expansion of preosteoblasts. *Cancer Res* 63, 5357-5362 (2003).

26 Ducy, P., Zhang, R., Geoffroy, V., Ridall, A. L. & Karsenty, G. Osf2/Cbfa1: a transcriptional activator of osteoblast differentiation. *Cell* 89, 747-754 (1997).

27 Stock, M. & Otto, F. Control of RUNX2 isoform expression: the role of promoters and enhancers. *J Cell Biochem* 95, 506-517 (2005).

28 Olson, E. N., Arnold, H. H., Rigby, P. W. & Wold, B. J. Know your neighbors: three phenotypes in null mutants of the myogenic bHLH gene MRF4. *Cell* 85, 1-4 (1996).

29 Drissi, H. *et al.* Transcriptional autoregulation of the bone related CBFA1/RUNX2 gene. *J Cell Physiol* 184, 341-350 (2000).

30 Napierala, D. *et al.* Mutations and promoter SNPs in RUNX2, a transcriptional regulator of bone formation. *Mol Genet Metab* 86, 257-268 (2005).

31 Hall, B. K. Development of the clavicles in birds and mammals. *J Exp Zool* 289, 153-161 (2001).

32 Neve, A., Corrado, A. & Cantatore, F. P. Osteocalcin: Skeletal and extra-skeletal effects. *J Cell Physiol* (2012).

Acknowledgements

I thank Dr. Sato for everyday supervising and advising me. All of this research and my JSPS fellowship are indebted to him. I hope his and his family's, including two young children, happy growth in the future. I appreciate Dr. Nagatake for teaching me many of necessary experimental methods and comprehension of unhappy data. I thank Dr. Goto for inviting me to fascinating world of mucosal immunology. I appreciate Dr. Kurashima's cheering me up in all the time. I thank Dr. Okada for helping me starting my experiments and ES cell cloning. I appreciate Mr. Kaneto's contribution to me at the expense of his comfortable experimental circumstance. I would like to thank Ms. Arakawa, Mr. Minoda, Ms. Yoshida and previous my teammates for helping my lab life. I would like to give my sincere appreciation to my collaborators, Dr. Nakashima, Prof.Taniuchi, Prof. Yoshida and Prof. Takayanagi for sparing their precious time for my research and giving me a lot of instructive advices. I'm really grateful to Prof. Kiyono who let me decide my way by myself and kindly helped my life when I was troubles. At last, I would like to express my appreciation and regret for my family who always support me warmly.

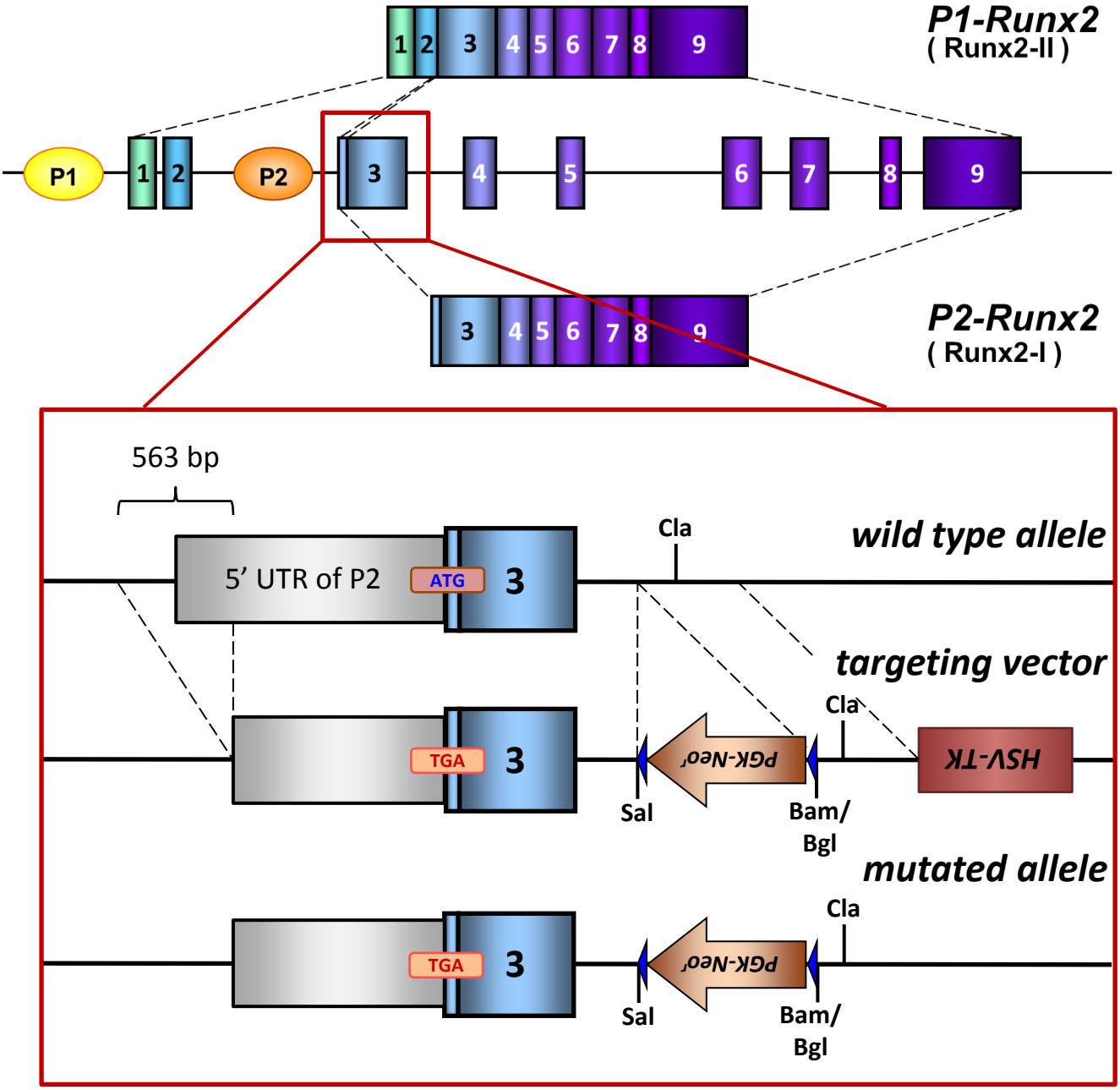

Figure1. A brief depiction of Runx2 gene structures and targeting strategy *Runx2* gene consists of two isoforms which are induced by different promoters and undergo alternative mRNA splicing. Both isoforms share over 90% of their coding region. The specific sequence for P2 isoform only exists in its 5' terminal. Therefore, this region was selected for gene targeting. The strategy was practiced by two manipulations: 1) mutation of first ATG of *P2Runx2* into TGA, the STOP codon. 2) deletion of 563 bp sequence including intron and 5' UTR of *P2Runx2*. Reverse oriented neomycin resistant gene cassette was inserted into the intron between exon 3 and 4.

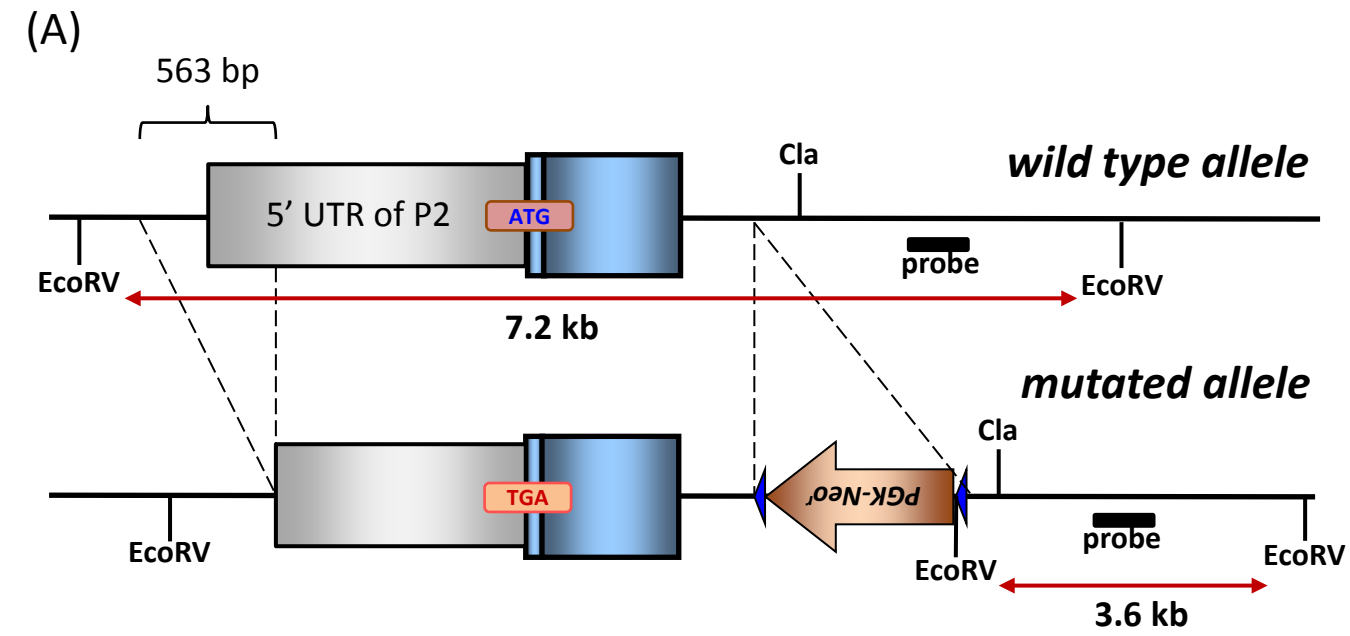

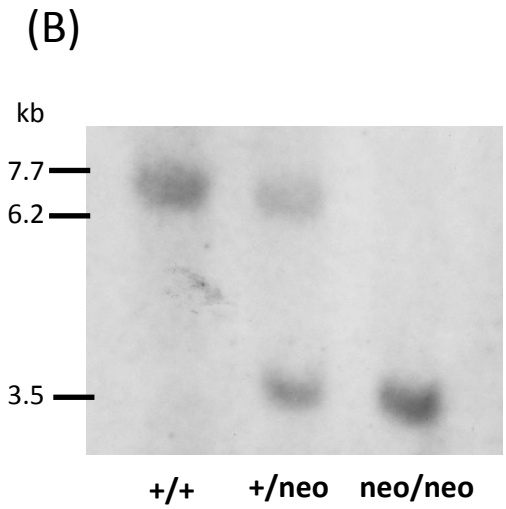

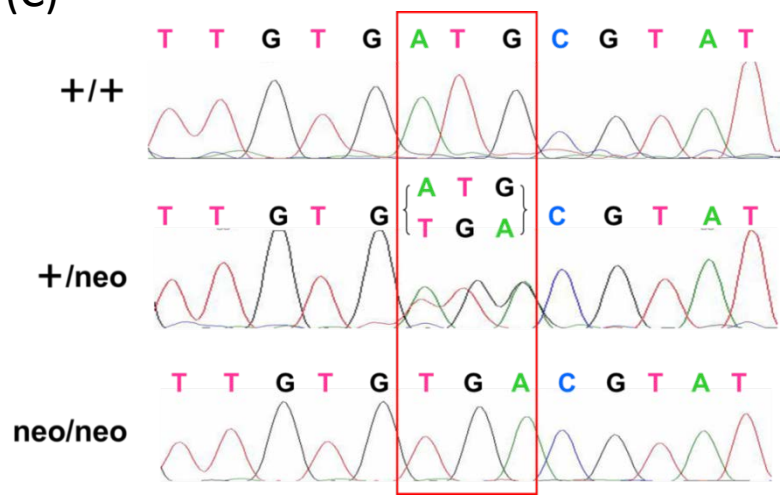

Figure2. Confirmation of gene modification A) Design of southern blot analysis . EcoRV recognition site was newly introduced into genome by accompanied with *neo*^{r} cassette. This EcoRV site would change the length of EcoRV digested fragment in which probe was settled. Thus, wild type allele would provide 7.2 kb fragment whereas mutate allele would do 3.6 kb. B) Result of southern blot analysis. Genomes were digested by EcoRV and blotted by probe shown in (A). As expected, the probe hybridized to wild type allele at 7.2 kb and to mutated allele at 3.6 kb. C) Gene sequence analysis against first ATG of *P2Runx2*. The genome was amplified by PCR with primers flanking this region and the PCR product was read by sequencer directly. This resulted in the ATG peaks in wild type, TGA peaks in mutant and TGA peaks as strong as ATG peaks in heterozygote.

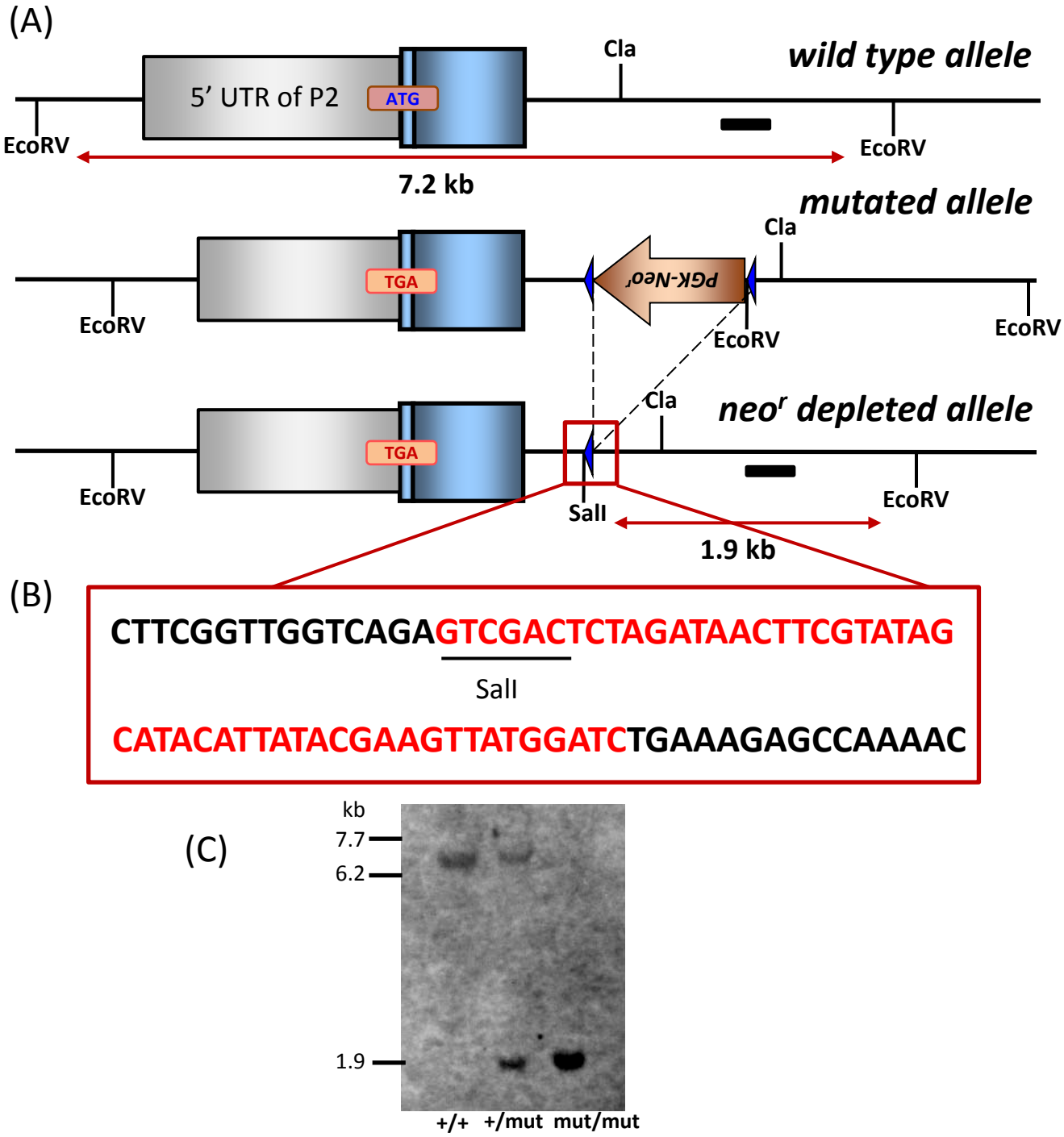

Figure3. *Neo*^{r} deletion and confirmation of it. A) Brief illustration of *neo*^{r} depletion followed by southern blot confirmation. After Cre-loxP excision, there would be remnant of loxP sequence containing SalI recognition site which was made use of for southern bolt analysis of *neo*^{r}-depleted mice. B) Nucleotide sequence of *neo*^{r} inserted site after depleting it. The sequence was amplified by PCR and the PCR product was subjected to sequence analysis. Letters marked by red color are nucleotides derived from loxP. The result showed the deletion of *neo*^{r} and existence of loxP remnant. C) Southern blot analysis was performed by double digested genomes by EcroRV and SalI and hybridized by probe shown in (A).

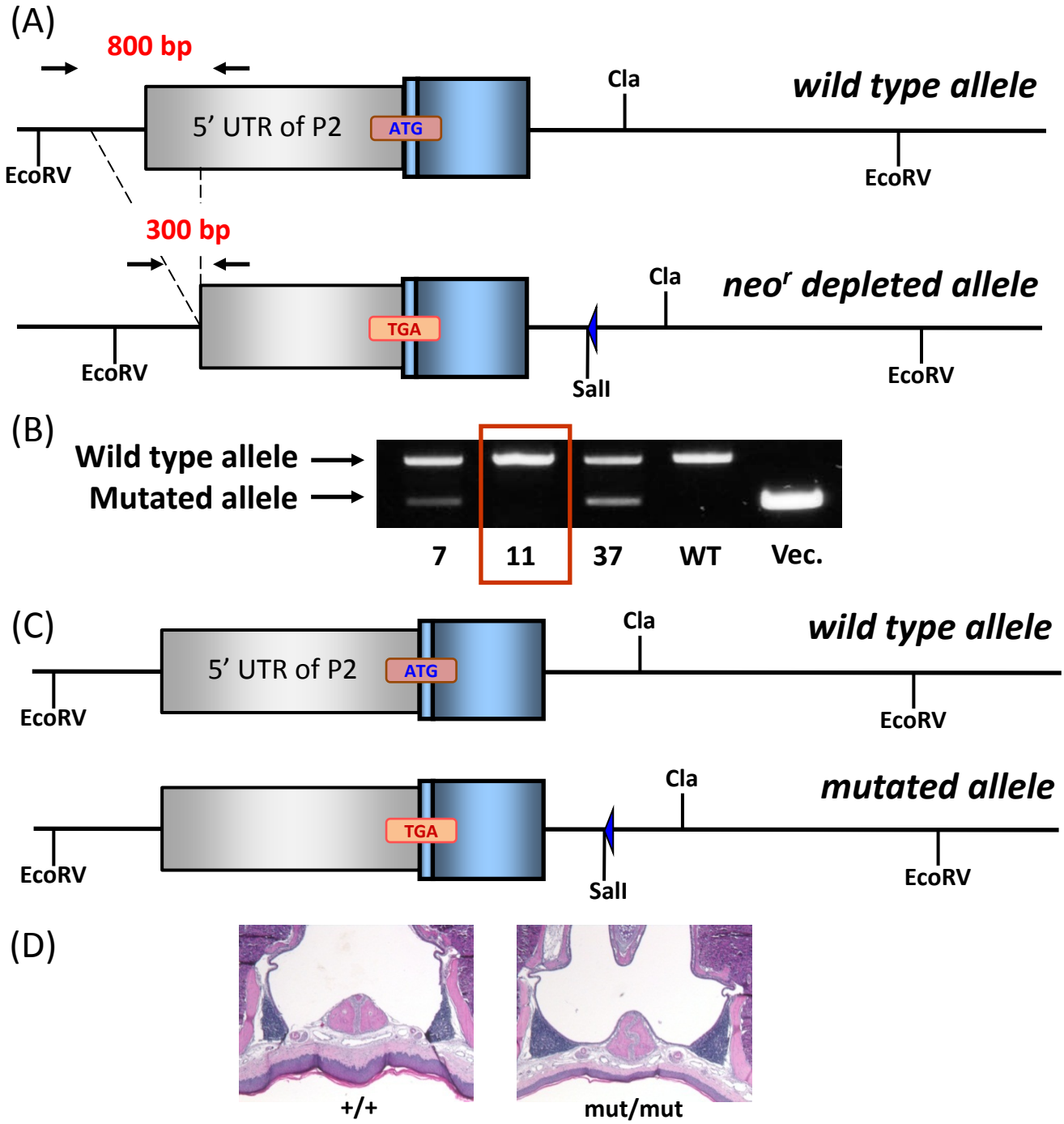

Figure4. 5' deletion was not accomplished and *neo*^{r} depleted mice had mature NALT structure. A) Illustration of the primer set that was designed to detect the deletion sequence. PCR performed by the same primer set would provide product of approximately 800 bp from wild type allele and 300 bp from mutated allele. B) The result of PCR performed by using ES cell genome as template. The result clearly showed incomplete targeting vector recombination in ES cell line #11. Number is clone name of ES cell line and "Vec." means targeting vector as template of PCR. C) The final version of description of mouse genome construct based on results of experiments. Mutated allele does not have deletion but possesses point mutation of *P2Runx2* first ATG to TGA. D) Tissue sections of *neo*^{r} depleted *P2Runx2* manipulated mice stained by hematoxilyn and Eosin. Homozygote mice exhibited mature NALT structure comparable to wild type littermate.

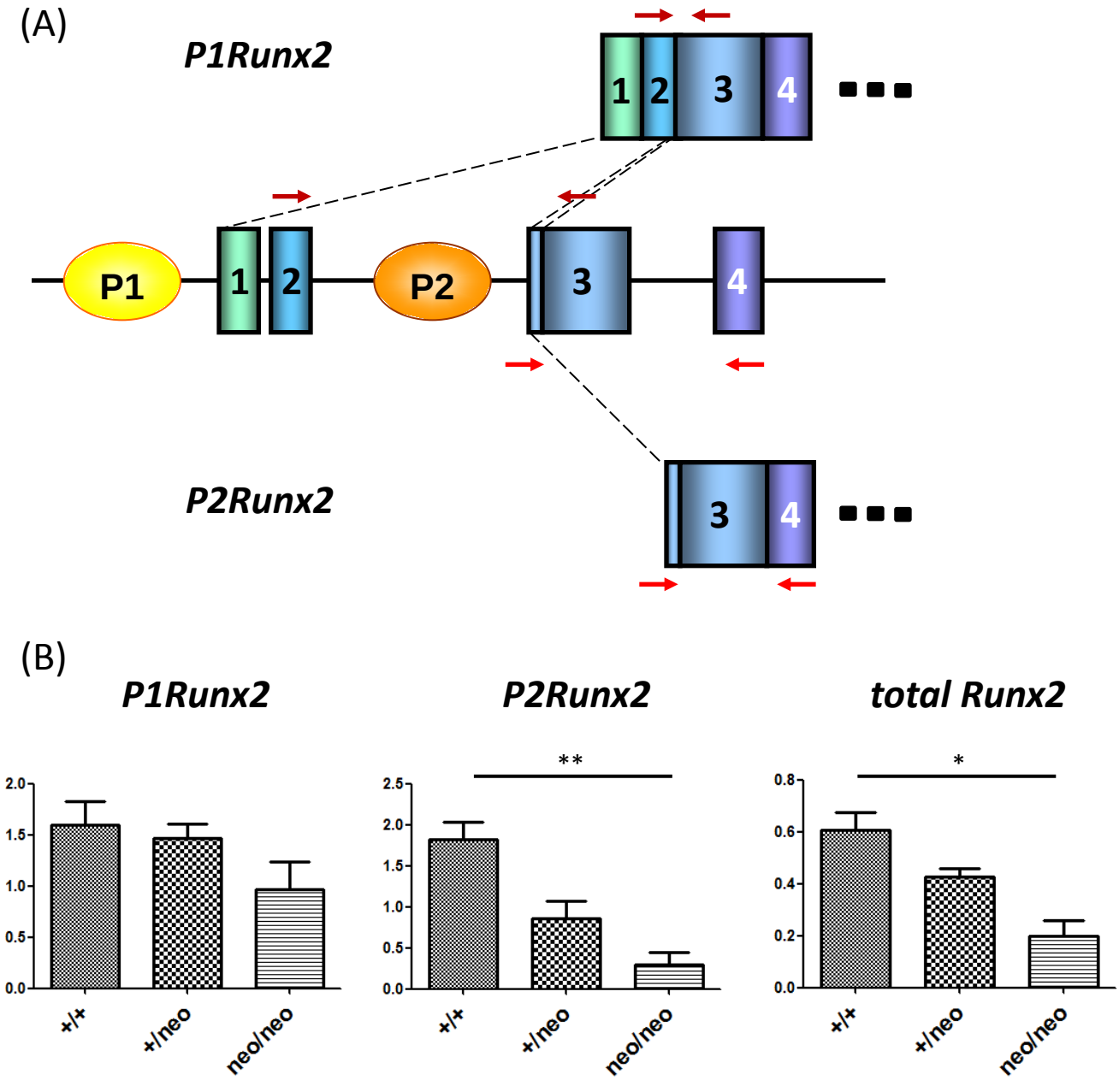

Figure5. Isoform specific quantification of *Runx2*. A) Isoform specific primers designed in this study was briefly described. Primers were set under the line (1) Use isoform specific 5' exons for each *Runx2*. (2) Forward and Reverse primers should put in different exons so as to flank spliced-out intron. Following these rules, primers were designed as shown in (A). B) Result of quantitative real-time PCR performed with SYBR green. Templates were prepared from E18.5 calvarial cells and reverse transcribed by using oligo dT primer. While *P1Runx2* did not show significant difference among three genotypes of mice, *P2Runx2*$^{neo/neo}$ mice exhibited significantly lower amount of *P2Runx2* gene transcript compared to wild type litter mates. Consequently, total *Runx2* transcript was also decreased significantly in homozygote mice.

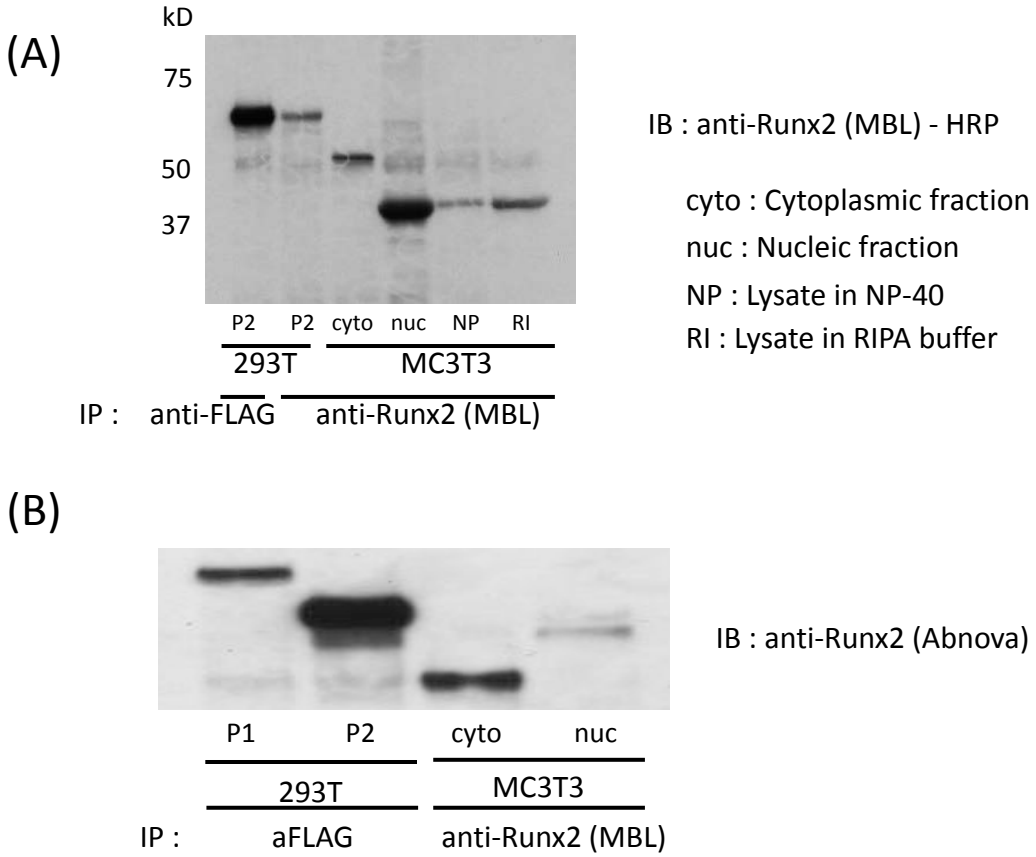

Figure6. Trials of western blotting were not successful due to low affinity of antibodies. A) Result of western blotting. The membrane was blotted by anti-Runx2 antibody (purchased from MBL) labeled by horse radish peroxidase (HRP). Positive control sample was prepared from HEK 293T cells transfected with FLAG-tagged murine P2Runx2 expression vector. Therefore the protein could be immunoprecipitated efficiently by anti-FLAG antibody (clone: M2) shown in the far left lane. The same sample immunoprecipitated by anti-Runx2 antibody (MBL) showed much weaker signal strength (lane 2), estimated lower than the half of left lane. This means the efficiency of I.P. by this antibody, which can be used for I.P. of endogenous protein, is extremely low. In consistent with this notion, endogenous Runx2 protein from MC3T3 pre-osteoblastic cell line, which expresses high amount of Runx2 in gene transcription level, could not be detected in this experiment. Since Runx2 is a transcription factor which should localize in nuclei, nuclear protein was extracted from this cell line beside the cytoplasmic contents. The attempt was not fruitful to give positive result. B) P1Runx2 protein, in addition to P2Runx2, was prepared by forced expression system against HEK 293T cells. FLAG-tagged recombinant proteins were concentrated by immunoprecipitation against FLAG tag and the signals of them were compared from those of endogenous ones expressed in MC3T3 pre-osteoblast cell line. The antibody (MBL) was used in the previous report s. They explained both P1 and P2 Runx2 were detected in different band as seen in the far right lane. And they claimed that upper band is obtained from P1 isoform and lower from P2. But recombinant positive control signals appeared at location far from them, especially in case of P1. Since I could not address this contradictive issue more precisely and could not solve the problem of low detective efficiency, I quitted this western blot examination which was necessary for the confirmation of existence of truncated form *P2Runx2*$^{mut/mut}$ mice. I suppose, based on my data, that the two bands reported previously were both P2Runx2; one was full length of it and the other is truncated form of it lacking the exon6 by frequently observed alternative splicing.

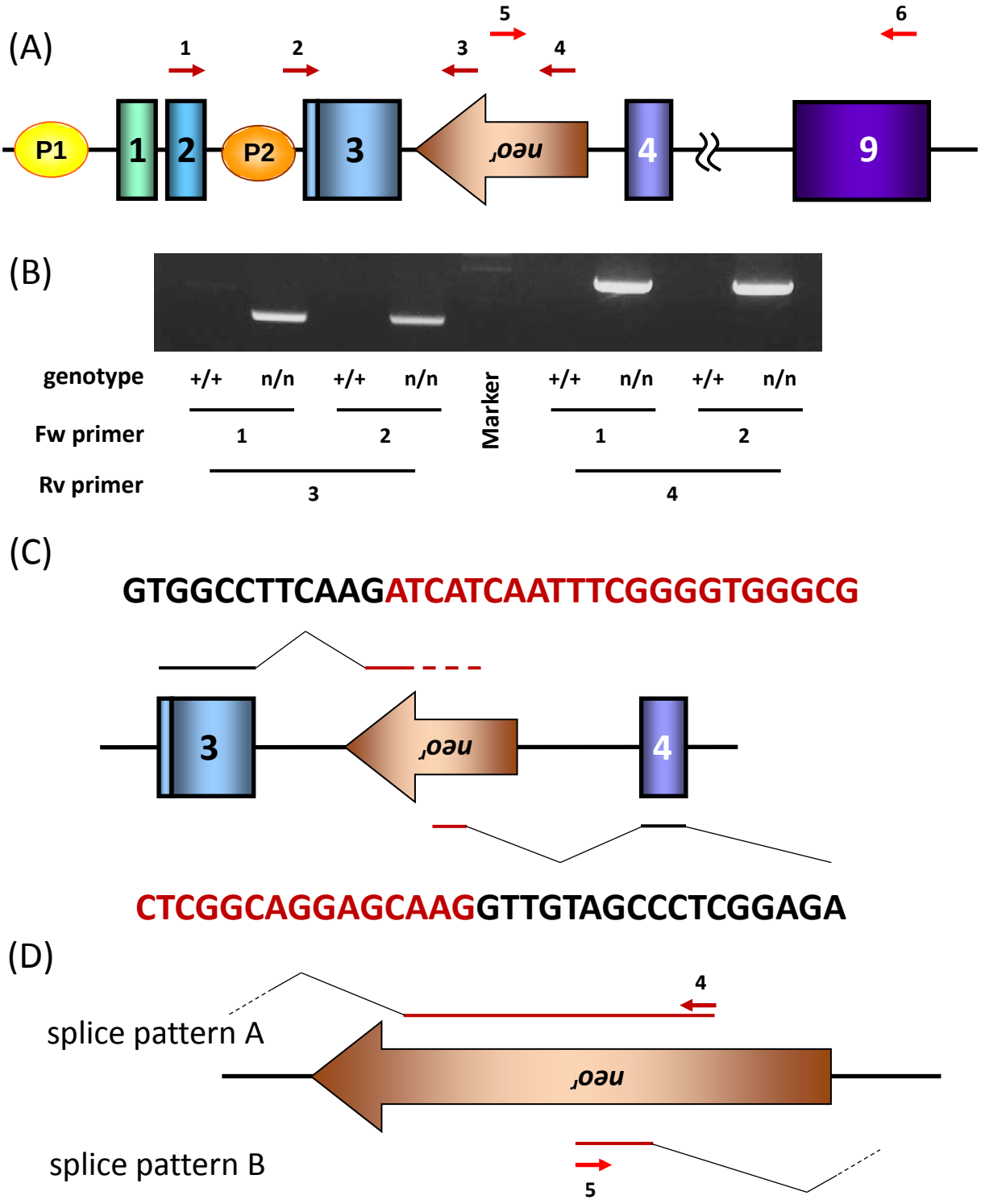

Figure7. *Runx2-neo*^{r} fusion transcripts were generated. A) A brief description of locations of primers for PCR amplification. B) Result of PCR. C) PCR products were subcloned and sequenced. Letters marked by red color were nucleotides derived from *neo*^{r} cassette. Splicing sites were briefly illustrated based on the sequence results. D) Two splicing patterns were briefly depicted for comparison. Considering results of successful amplification by primer 4, RNA shown as top in (C) is assumed to be pattern A. In contrast, RNA shown as bottom in (C) was revealed to be pattern B by sequencing. Therefore, there should be at least two different types of irregular splice product. But *neo*^{r} internalized type of variants were not detected.

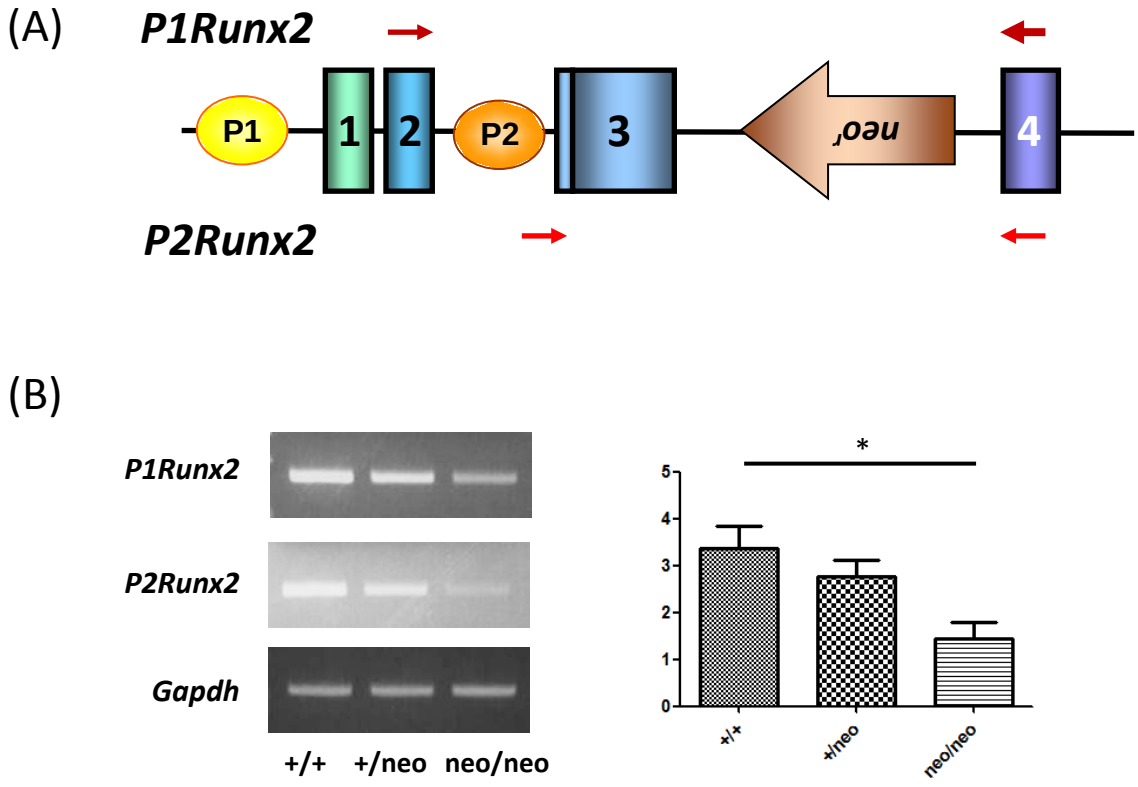

Figure8. Modification of qPCR design for *P1Runx2* revealed diminished P1 transcripts. A) The reverse primer for qPCR of *P1Runx2* was changed from that shown in Figure5. to make the primer set flank the intron between exon3 and 4. Moved primer is marked by larger size than others. B) Result of quantification of *P1Runx2* by modified primer set. Both in semi-quantitative PCR and quantitative PCR, the amount of *P1Runx2* transcripts was substantially and significantly decreased.

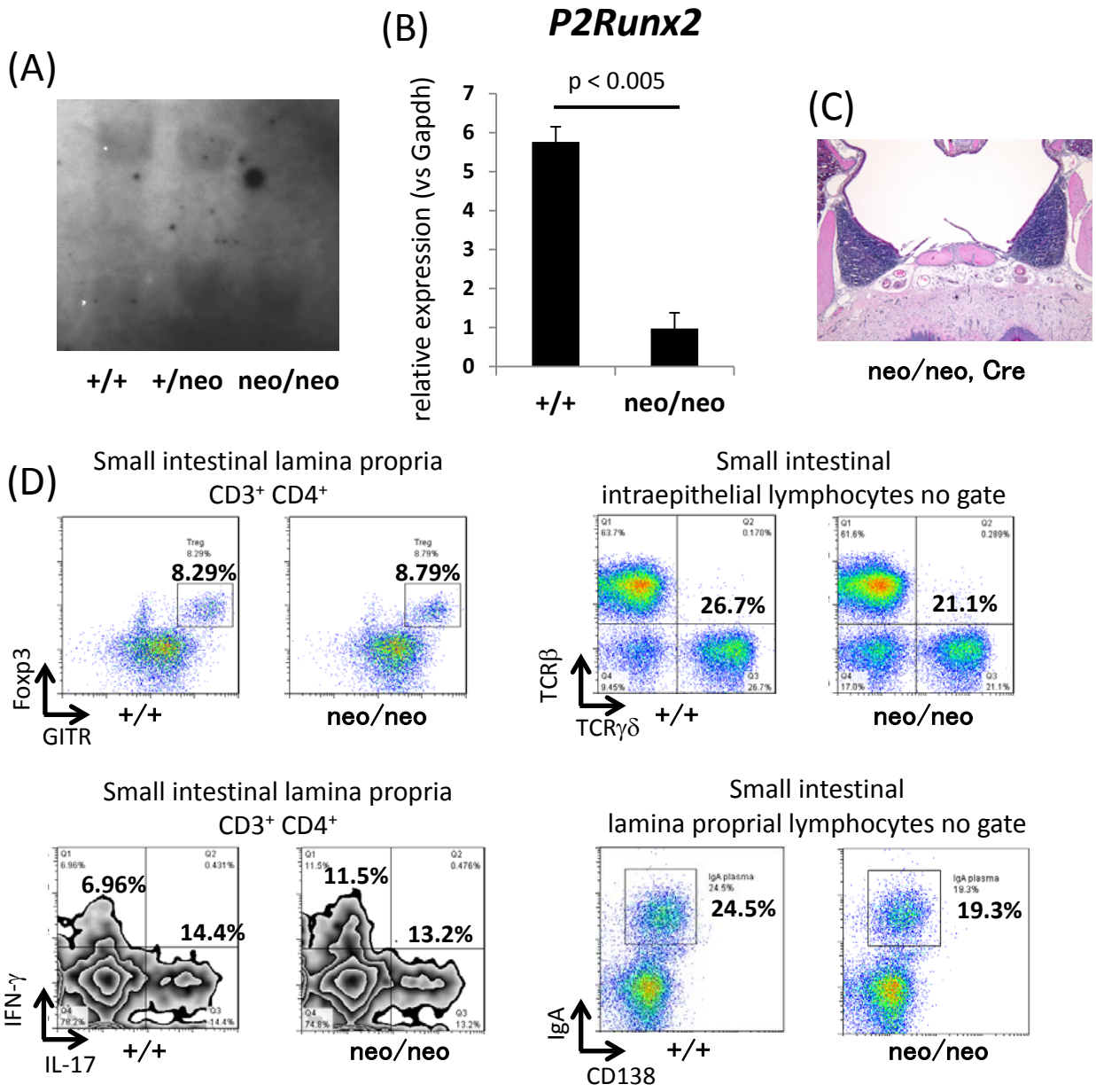

Figure9. Col2a1-Cre/*P2Runx2*$^{neo/neo}$ mice showed no immunological phenotype. A) Southern blot analysis performed by tail lysate of Col2a1-Cre/*P2Runx2*$^{neo/neo}$ mice. All of mice used here possessed Cre transgene. The design of southern blot was same as Figure 2 (which was designed for *P2Runx2*$^{neo/neo}$ mice). The result showed that the adult mouse had *neo*^{r} alleles for homozygote, which means this mouse overcame *neo*^{r} lethality. B) mRNA was prepared from splenocytes of Col2a1-Cre/*P2Runx2*$^{neo/neo}$ and wild type littermate, showing significantly decreased amount of *P2Runx2* transcript in homozygote mice. C) Tissue section of Col2a1-Cre-*P2Runx2*$^{neo/neo}$ mouse stained by hematoxilyn and Eosin. D) Series of FACS analyses focused on immunological function of Col2a1-Cre/*P2Runx2*$^{neo/neo}$ mice. Designated cells were prepared and stimulated *ex vivo*, if it was needed, and then analyzed by FACS Calibur. All of results showed comparable cell differentiation between wild type and homozygote.

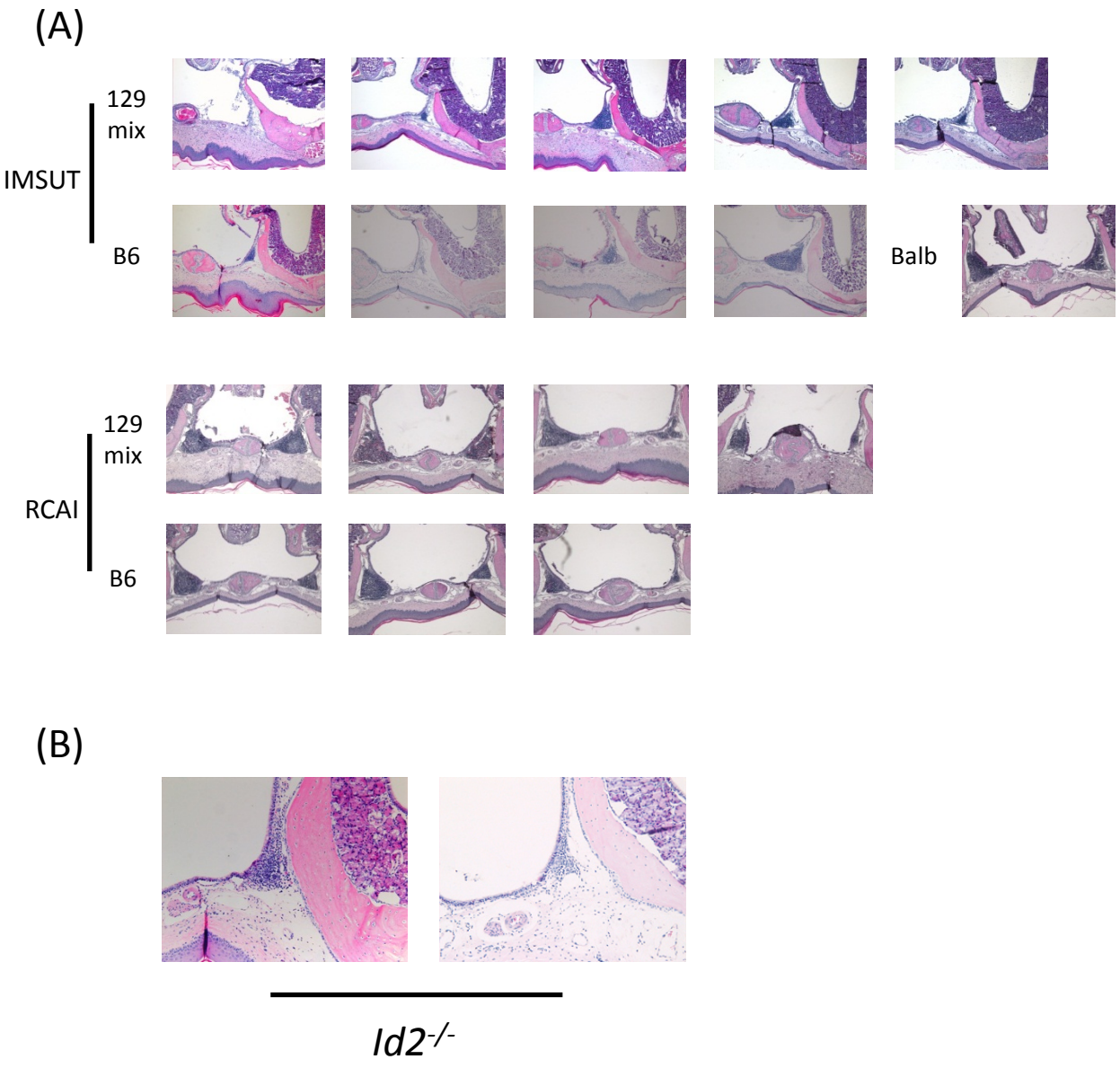

Figure10. A) Tissue sections of Cbfβ2 deficient mice, stained by Hematoxilyn and Eosin. Considerable number of mice, fostered in the facilities of Institute of Medical Science, University of Tokyo (IMSUT) and RIKEN Research Center of Allergy and Immunology (RCAI), were examined. It is true that some of them showed immature NALT formation, but most of them had well developed NALT structures regardless of the facility and of genetic background. B) Tissue sections of Id2 deficient mice stained by Hematoxilyn and Eosin. Because they can't produce homozygote pups under C57BL/6 background, mice were maintained as B6/129Sv mixed back ground (with dark grey fur). Knockout mice showed small, but obvious NALT-like structures in contradiction with previous results.

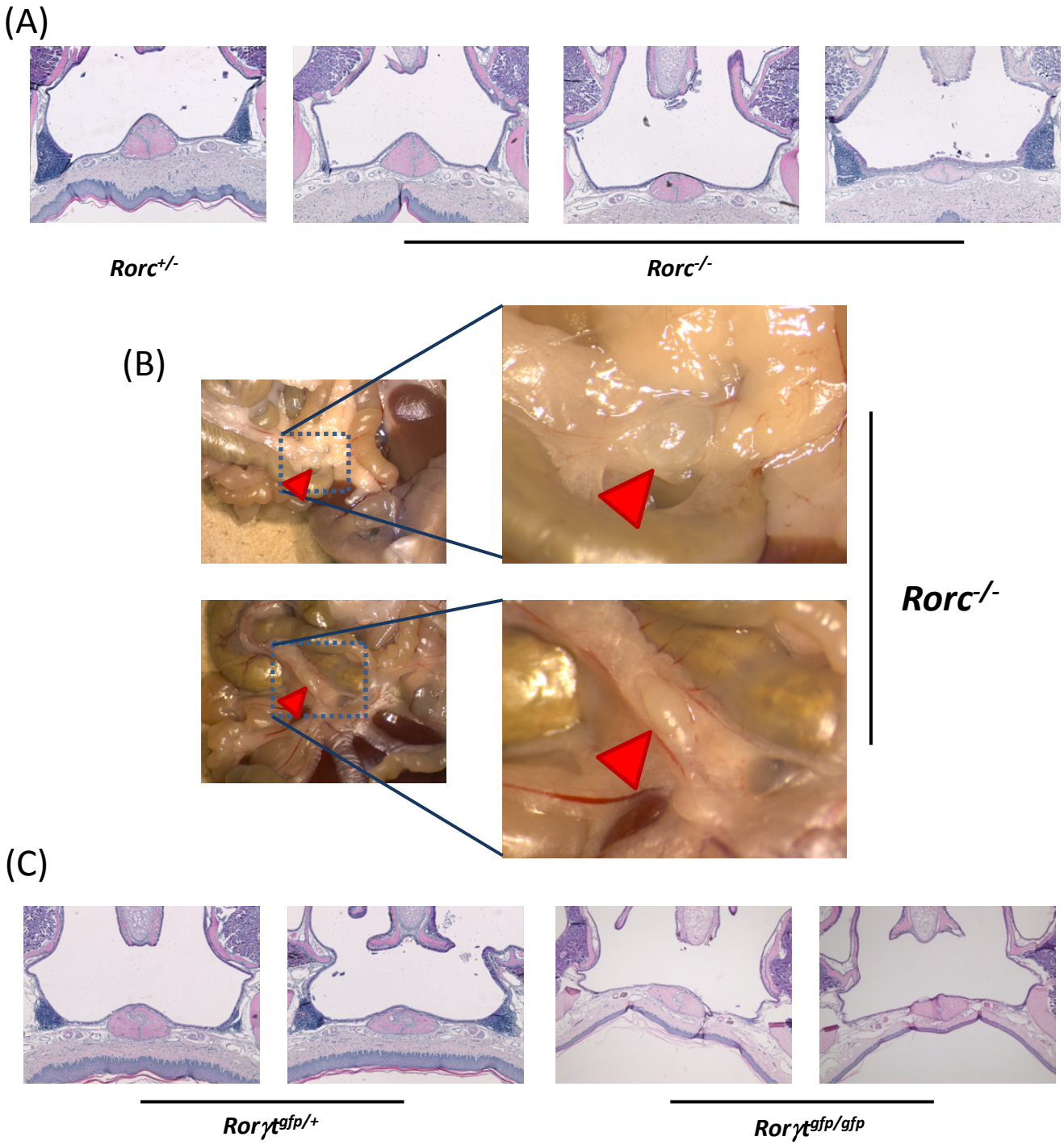

Figure11. *Rorc*$^{-/-}$ and *Rorγt*$^{gfp/gfp}$ mice also showed incompatible results with previous reports. A) Nasal tissue sections of RORC knockout mice were stained by Hematoxilyn and Eosin. Two of three RORC deficient mice showed diminished NALT structure. Mature NALT structures observed in heterozygote mouse verified that the experiments were performed orthodox methods. B) Lymph node like aggregations were found in RORC knockout mice mesentery. Lower (left) and higher (right) magnifications, in which lymphoid tissue-like structures were marked by red arrowheads, are shown. In lower left panel, the structure locates in the center of mesentery, which is different from the localization of FALC. C) Tissue sections of isoform specific RORC deficient mice (*Rorγt*$^{gfp/gfp}$) were staining by Hematoxilyn and Eosin. Again, the sections of heterozygote verified the orthodox method used in this experiments.

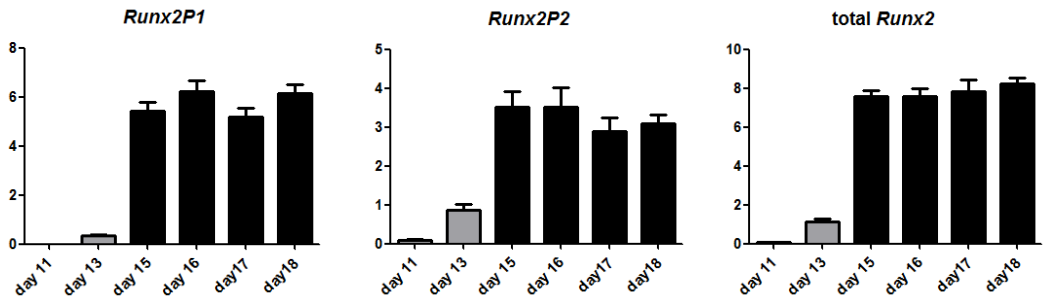

Figure12. Calvarial *Runx2* expressions are stable during embryonic stages. Expression profiles of *Runx2* isoforms and total *Runx2*. Calvairal tissues were digested by collagenase and dispase to purify clavarial cells of fetus. In embryonic day 11 and 13, however, calvaria were not formed yet. Therefore, whole upper head tissues were lysed to extract RNA, instead. RNAs were reverse transcribed with oligo dT primer and their amounts were evaluated by quantitative real time PCR with SYBR green system. Expression of each isoform was normalized by the expression of *Gapdh*.

	P1	P2	total
+/+	1	1	1
+/neo	0.82	0.47	0.70
neo/neo	0.42	0.16	0.33

$$\frac{0.42(1+x)+0.16}{(1+x)+1}=0.33 \quad \cdots\cdots (1)$$

$$x=0.88$$

$$2alleles\times P1Runx2+2alleles\times P2Runx2=totalRunx2 \quad \cdots (*)$$

$$2\times 1.88y+2\times y=100 \quad \cdots\cdots (2)$$

$$y=17.2$$

Table1. Relative decrement of *Runx2* in *P2Runx2*$^{neo/neo}$ mouse and calculation of ratio between P1 and P2 isoforms. The expression level of each isoform and total *Runx2* of each genotype mouse shown in figure5 and 8 are presented again in ratio to the wild type. When the decrement of total *Runx2* is the average decrement of both isoforms, given x as the ratio of how more *P1Runx2* is expressed than P2 counterpart, the equation (1) holds. Solving this, *P1Runx2* is expressed about 90% more than *P2Runx2*. Next, considering total *Runx2* is given by addition of P1 and P2 *Runx2*, the equation (*) holds. Given y as contribution of one allele of P2 isoform for total *Runx2* (100%), the equation (2) holds. Solving this, the contribution of one copy of P2 isoform is 17.2% and then P1 isoform is calculated as 32.8% in E18.5 calvaria.

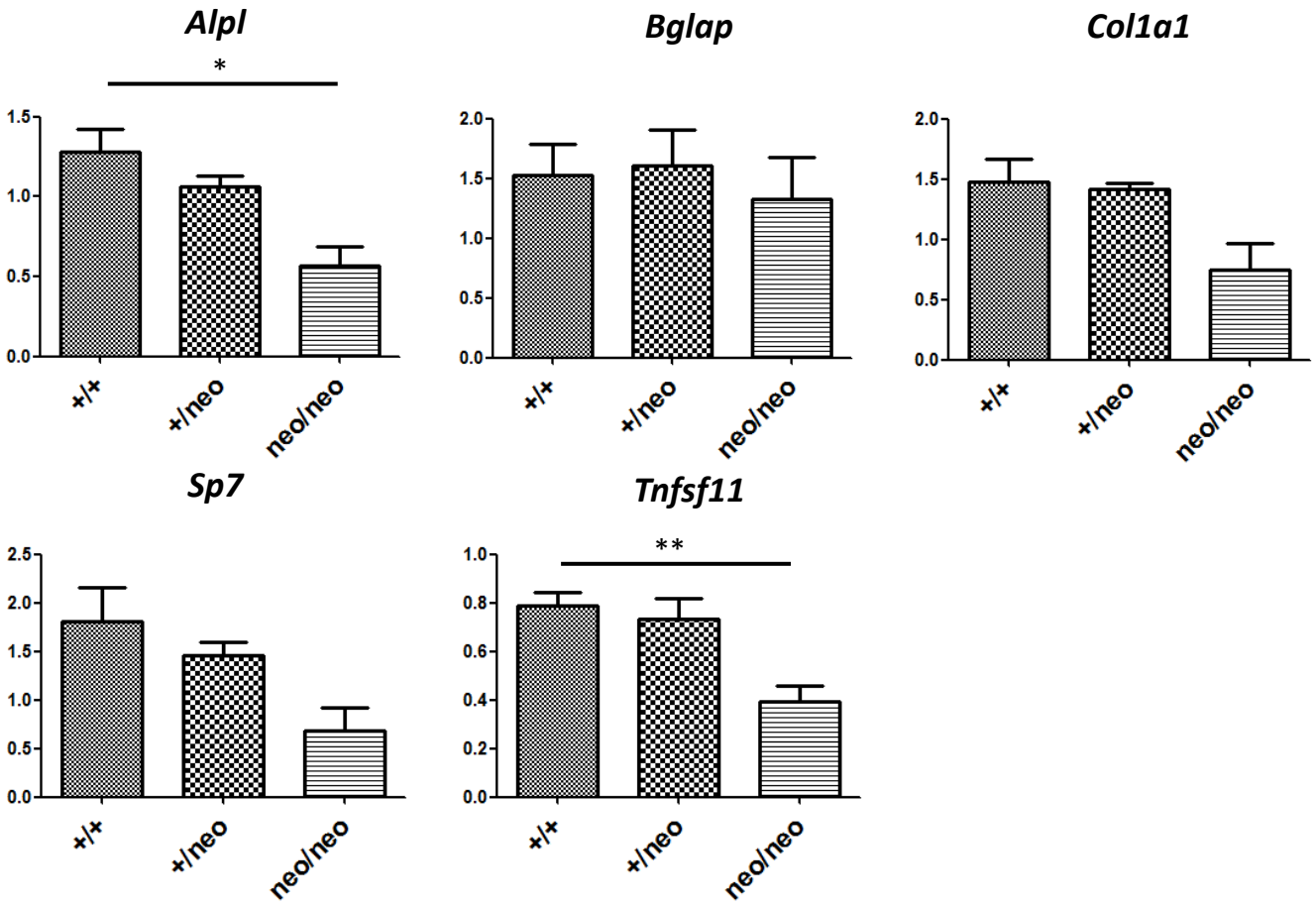

Figure13. Osteogenic gene expressions were decreased in *P2Runx2*$^{neo/neo}$ mice.
Osteogenic gene expression profiles of *P2Runx2*$^{neo/neo}$ mice were examined. Calvarial cells were purified from fetus at embryonic day 18.5 and lysed to extract RNA. RNAs were reverse transcribed with oligo dT primer and the amounts of gene transcripts were evaluated by quantitative real time PCR with SYBR green system.

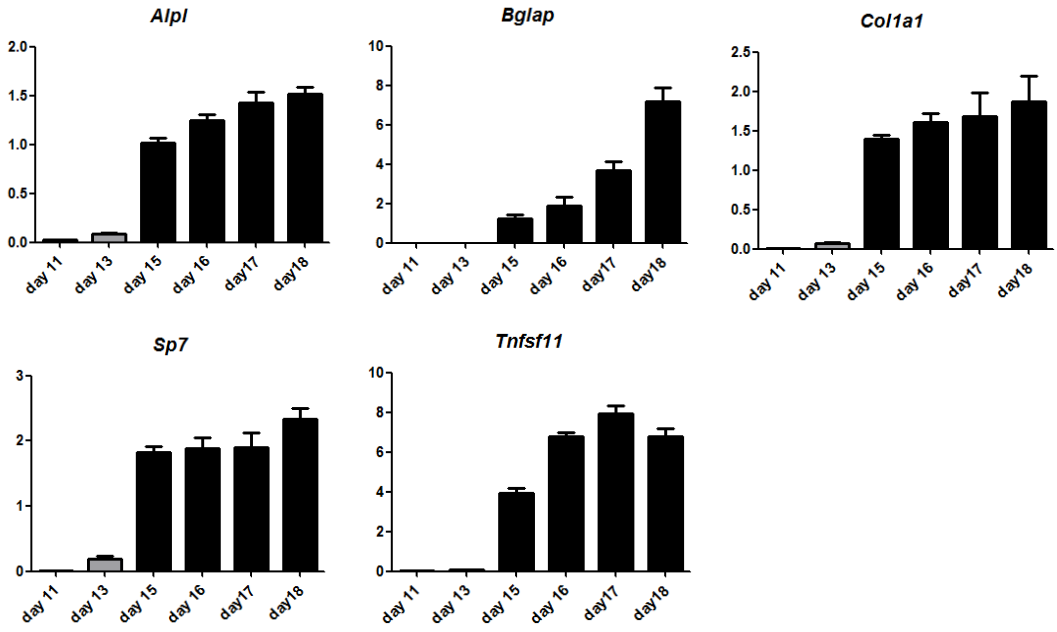

Figure14. Osteogenic gene expression during embryonic development. Transcripts of designated genes were quantified by using the same samples as Figure10. The number of samples in each group is 7-9.

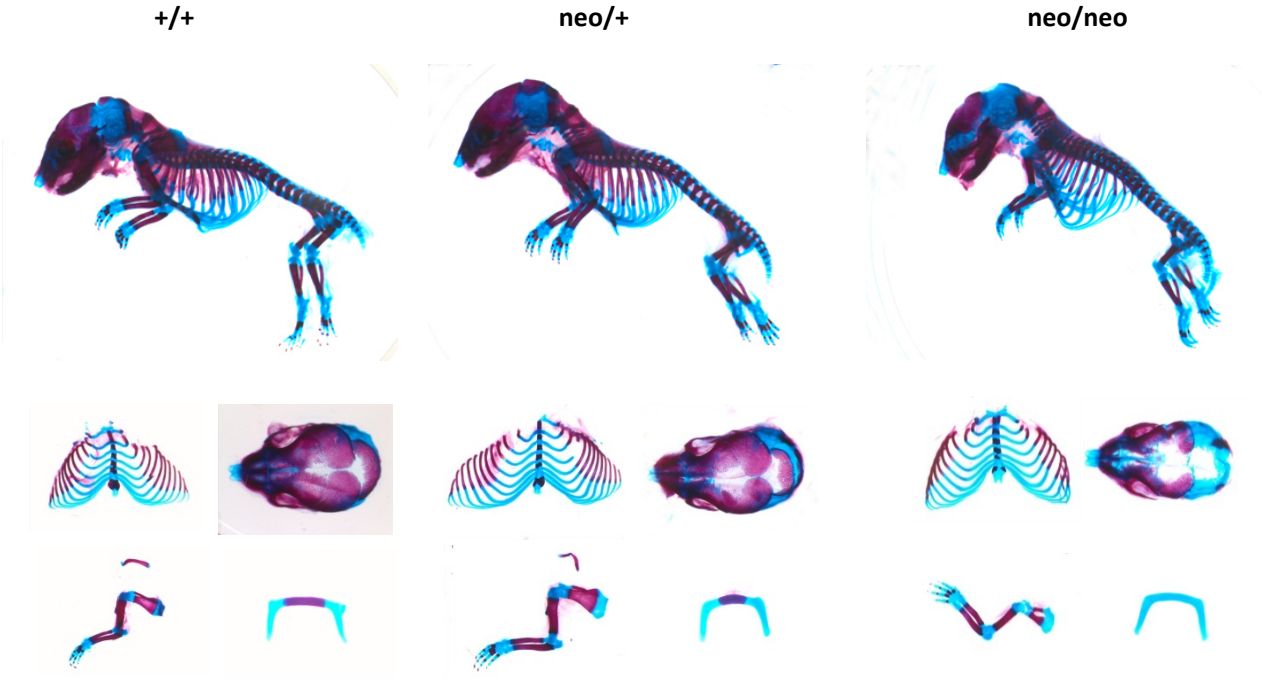

Figure15. *P2Runx2*$^{neo/neo}$ mice delayed bone formation. Skeletal specimens were prepared from *P2Runx2*$^{neo/neo}$ mice and their littermates and stained by Alizarin red and Alucian blue. Whole skeletons and each part were shown.

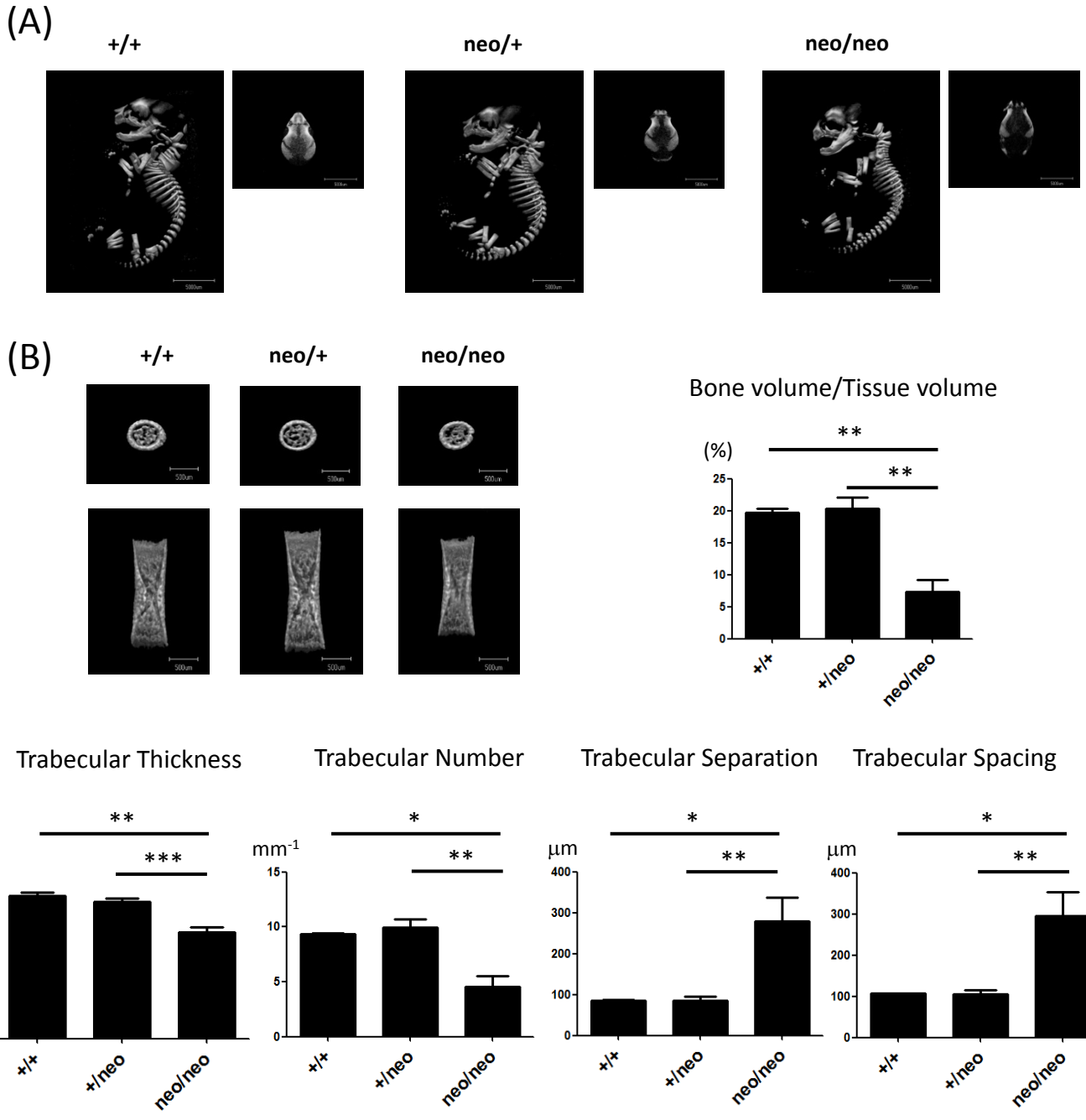

Figure16. **Ossification of *P2Runx2*$^{neo/neo}$ mice was significantly delayed.** micro CT analyses of *P2Runx2*$^{neo/neo}$ and littermates. Their whole skeletons and skulls were scanned, and their femurs were subjected to the quantitative evaluation. (A) Views of whole skeleton and skull are shown. (B) Figure of femurs and calculated parameters are shown.

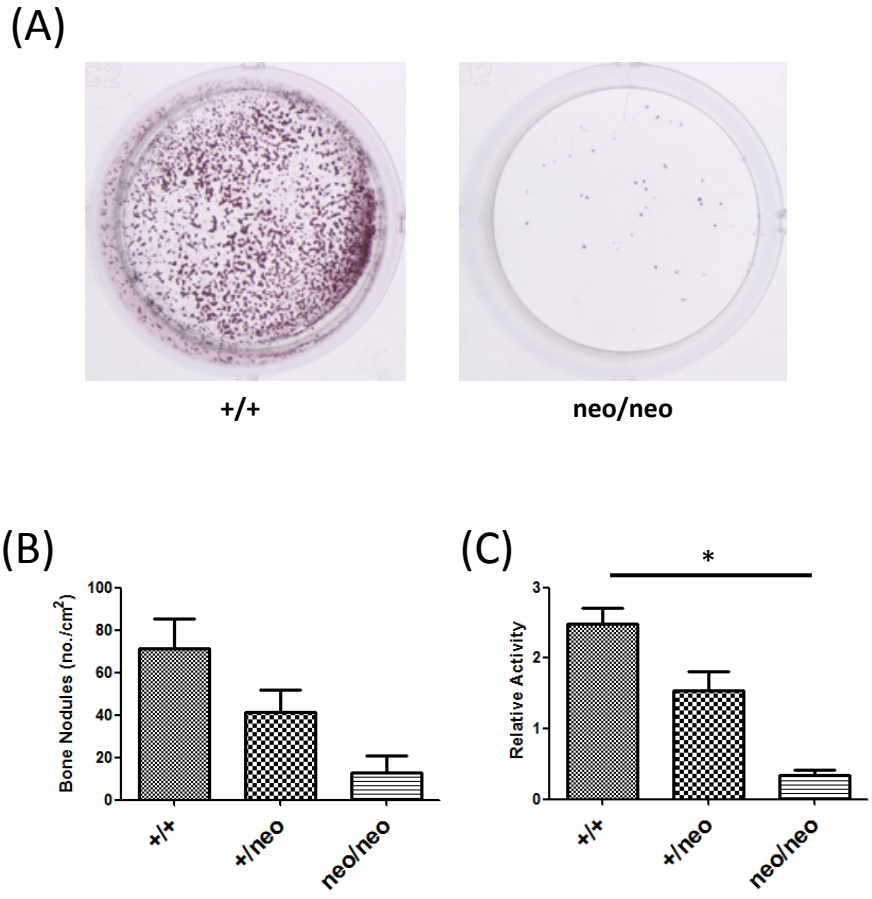

Figure17. Delayed bone formation of *P2Runx2*$^{neo/neo}$ mouse is the consequence of defective osteoblast development. Fetal calvarial cells were purified from embryonic day 18.5 fetuses and cultured in the osteoblast developmental medium for two weeks. A) After the culture period, the culture plate was stained by Alizarin red. Representative staining patterns are shown here. B) The number of one nodules shown in (A) was counted. C) At the same time as bone nodule evaluation, cells were lysed to examined Alkaline phosphatase activity. Activity was measured as degradation speed of p-nitrophenylphosphate determined by absorption of wave length 405 nm.